4-27-2010

Improvement of the Gait Analysis Process

Michael Brothers
Trinity University

J. Dizon
Trinity University

Zachary Kammer
Trinity University

Alexandra Leamy
Trinity University

K. Poole
Trinity University

TRINITY UNIVERSITY

Improvement of the Gait Analysis Process

ENGR-4381

4/27/2010

Senior Design Project - GAIT

M. Brothers, J. Dizon, Z. Kammer, A. Leamy, K. Poole
Dr. Uddin, Advisor

Pledged

Kristin Poole Michael Brothers
Zachary Kammer

This report describes the complete design and testing of a methodology for the creation of a force sensing device that can be used to provide clinically significant data to aid a prosthetist in the static alignment of a transtibial prosthesis fitting. Thin-film force transducers form the basis for the prototype force sensing module that is integrated into a prosthetic leg for the testing and future alignment fittings. This physical force sensing device was used along with a computer simulation of the limb and module to collect force measurement results, both positionally relative and absolute. The experimental data collected were analyzed using Analysis of Variance, effects plots and prediction equations. The statistical analysis helped to evaluate the feasibility of using similar data and methods for producing a system capable of predicting and validating changes in force distribution based on changes in alignment in a clinical setting. While both the computer simulation and physical force sensing device were able to detect the same trends in the alignment/force distribution relationship, the accuracy of the force sensing module could be improved. The recommendations for future revisions of this design include using more accurate force sensors and conducting more replications of the physical testing.

Executive Summary

Observational Gait Analysis (OGA) for amputees with prosthetic limbs is still the primary method used by clinicians worldwide even though it has been shown to be less repeatable than the much more expensive computerized gait analysis. OGA helps the clinician find the optimal alignment for a patient through knowledge of a clinically accepted initial alignment followed by observation of the patient ambulating with the prosthesis.

In the average prosthetics facility, direct measurements of forces, stress, strain and torque are not available. Instead, a prosthetist must rely on a "trial and error" approach with patient feedback and subjective observation to optimize the patient's gait through proper alignment. Therefore, there is a need for an improved procedure for prosthetic alignment that is financially feasible for an average prosthetic facility. The objective of this particular project was to design and develop a method for obtaining quantitative measurements of forces on a prosthesis. The force distribution information produced in a data output system was used to help a prosthetist better understand the loading on the limb as well to help make suggestions for possible alignment changes.

Small, thin-film sensors known as FlexiForce force sensors, made by Tekscan, were selected as the basis of the force sensor system for this design. These piezoresistive sensors were incorporated into a component that was integrated into the prosthesis just below the socket. The sensors measure a force through a change in resistance. The resistance values of the sensors served as inputs to a data output system. With the data output system, the user can enter the sensor resistance values into a spreadsheet program and receive quantitative information about the force distribution on the prosthesis. The program also contains suggested alignment adjustments that may help speed up the process of finding the optimal alignment.

The force sensing system and transtibial prosthesis were modeled in ProMechanica so that computer simulations of many different alignment and loading scenarios could be conducted in parallel with physical testing. The results of the computer simulation and tests on the physical prototype were compared and used to create effects analysis graphs in Minitab, which served as confirmation of physical intuition for the test results. The Minitab analysis was also used to develop prediction equations based on the coefficients produced and the corresponding p-values that make a case for the statistical significance. Results were mixed; while it was clear from

pg.

statistical analysis that there was an identifiable correlation between alignment and force distribution, the force sensors employed in the design could not offer accurate measurements due to a lack of sensor sensitivity and an inability to measure tension forces. Ultimately, these results serve as an indication for the potential in this line of research. We recommend that sensors which can more accurately measure the applied forces be used for future revisions on this design. Then the methodology devised in this project would likely culminate in a cost effective quantitative system for force analysis that would be of great benefit to patients and practitioners.

Table of Contents

Table of Figures

Table of Tables

1 Introduction

This project was intended to address the need in the field of prosthetics for more cost effective and scientific procedures for prosthesis alignment. The following sections provide relevant background information that illuminates this need as well as a description of the objectives of this project.

1.1 The Field of Prosthetic Limbs and Gait Analysis

The need for prosthetic limbs has been around for thousands of years, dating all the way back to rudimentary wooden peg legs. As the years have passed, these simple and archaic substitute limbs have been replaced by more functional and advanced prostheses. While great changes have occurred in the development of the actual prosthesis, the stigma often associated with having a missing limb as well as the self-consciousness of the amputee has remained relatively unchanged throughout many of these advancements in history. However, as cultural mentalities have shifted to become more accepting and inclusive, these problems have somewhat started to diminish. Medical advances that can now save the lives of critical patients through sophisticated surgical techniques have contributed to a population of amputees who want to continue their previous active lifestyles and have created a demand for highly functional limbs. This is especially true in the military, where dangerous combat situations have left many young and active men and women with missing limbs in the past decade.

As a result of these factors, there has been a substantial and significant improvement in the technological design of prosthetic limbs in the past few decades. New fabrication and fitting techniques have helped vastly improve the look and feel of the limbs for the users. Computerized "smart" limbs are being developed to move closer towards mimicking the functional abilities of the flesh-and-blood human limb. While technological progress in prosthetic design is fantastic, if the device does not fit the patient or function correctly, then all of the cutting-edge advancements go to waste.

For a unilateral transtibial (below the knee) prosthesis specifically, creating a properly functioning prosthesis means that proper gait and alignment are of the utmost importance in order to guarantee that these high tech prosthetic devices perform optimally. Gait refers to the manner in which a person moves, such as stride distance and angle of heel strike. It is very

important that the gait of a patient using a prosthetic leg be kept as identical as possible to the gait of a non-amputee in order to ensure the well being of the patient's remaining limb. As described previously, there has been a great deal of innovation in the design of the actual limb. However, there has been very little change in the methods for gait analysis in the clinical setting in the past 50 years (Boone 2009). The main technique used around the world during a clinical alignment appointment by a licensed prosthetist is called Observational Gait Analysis (OGA). For this technique, the prosthetist essentially uses all of the training he or she received through school and mentors, as well as personal experience, in order to make alignment corrections. The clinician observes the patient ambulating with the prosthesis and then uses his or her trained and experienced judgment along with knowledge of clinically accepted alignments in order to find the optimal alignment. However, this very popular and widely used technique has been shown to be less repeatable than computerized gait analysis (CGA) and yet still remains the primary method for fitting prosthetic legs. Improper alignment can result in skin breakdown due to excessive forces on the patient's residual limb and/or gait deviations that can cause both injury and unwanted attention to the amputee's missing limb.

There are several reasons that have prevented CGA from becoming a more commonly used technique in gait alignment. The biggest barriers have been CGA's time consuming process for fitting the prosthesis as well as the very high cost of the specialized facilities necessary to implement the technique. As a result, instead of the direct measurements of force, stress, strain and torque that would be provided for a clinician in a CGA lab, the prosthetist in an average clinical setting must use a "trial and error" approach. The clinician must rely on patients' feedback on what they are feeling as well as subjective observation by the prosthetist himself in order to try to find the optimal alignment. If a patient is unable to accurately interpret what he or she is feeling and/or unable to effectively communicate these feelings during the fitting, it becomes very difficult for the prosthetist to achieve a proper alignment.

1.2 Problem Description

All of this information exposes a significant need for developing an improved method for gait analysis and prosthetic alignment. The use of quantitative measurements of the forces on the limb as indicators of suggested alignment changes would help a prosthetist who currently uses OGA create a better alignment. The goal of this particular project was to create a device that

would help implement such an improved method by providing the clinician with objective and scientific data in a cost effective manner. The quantitative data would help the prosthetist find the optimal alignment during a static alignment in order to ensure a proper gait for a patient.

The primary objective of this project was to design and develop a new technique to obtain quantitative measurements of forces for prosthetic gait analysis. The technique was used to indicate alignment changes that would help improve the gait of a unilateral transtibial amputee. The goals of this design project also included a computer simulation of this technique. Considerable research and brainstorming among group members went into the design of the force sensing module. Several companies and research facilities have come up with concepts meant to provide the same type of data. Orthocare Innovations developed the Smart Pyramid™ to replace the standard pyramid in any prosthesis to allow for computerized gait analysis with its embedded sensors. The CompasMaster™ unit can then be attached to the pyramid in order to send the data to a computer that tracks the gait of a patient during dynamic alignment fittings. It then compares the data to curves describing "normal" gait in order to determine any gait deviations and indicate corresponding alignment changes that should be made (Orthocare Innovations 2009). However, the Compas system is extremely expensive and excessive for the measurements that this project intended to quantify during the static alignment phase of check socket fittings.

A scientific research paper for the Department of Veterans Affairs from the University of Washington Center for Bioengineering and Department of Mechanical Engineering was very informative. Sanders *et al.* discuss a similar project which used six strain gauges in a device to measure all of the force and moment components during walking. Then calibration curves and matrices were used to convert this data into force measurements (Sanders, et al. 1997). However, the authors do not go so far as to use the force measurements in order to make specific recommendations for alignments changes as this project does.

There were several constraints that influenced the direction of the design for this project. Economic issues are often significant factors in designs as engineers are always looking for better and cheaper ways to accomplish a job and this project is no exception. The device needed to provide a cost effective alternative to computerized gait analysis (CGA) in order to appeal to prosthetists who are working in an average prosthetic facility. The average prosthetist does not have the access or the financial means for high tech gait labs. Although the budget supplied by

Trinity was $1,200, a practicing prosthetist and technical consultant for this project, Tiffany Forest, suggested additional cost guidelines for the actual device in order for it to be a cost effective design. It was recommended that the force measuring device should not exceed $150 if it is to be used fewer than five times, but it may cost up to $500 if it can be used more than five times. Since the group unanimously decided that the device should be designed to be used many more than five times, the goal was to provide a product at a cost of $500 or less to a prosthetist.

Health and safety were also very important constraints to consider, especially when dealing with a human being's reliance on the device functioning properly to remain safe. Any prototype and final product that is incorporated in the prosthesis fitting process must not compromise the integrity of the original prosthetic limb or the safety of the patient in any way. It should also be compatible with the materials and strength of the prosthesis in order to meet this constraint.

2 Design Overview

All of this information, along with a great deal of background research, provided an excellent foundation for choosing the design that best fit the stated objectives of this project. The major systems within the design solution for this problem were the force sensor system, the data output system, and the computer simulation. A testing apparatus was necessary but was not considered part of the final deliverable. The force sensing device that was selected to solve this problem consisted of a set of four Tekscan FlexiForce sensors mounted between two metal plates. The sensors (Figure 1) were thin-film, piezoresistive sensing devices containing a flexible printed circuit. The sensing area (circular area at the end) senses a contact force, causing silver to extend from the sensing area to the connectors at the other end and the resistance of the sensor to change (Tekscan 2007). The connectors at the end of the sensor served as the connection between the force sensor system and the data output system. The force measuring component was placed between the socket of the prosthesis and the pyramid that is connected to the pylon as shown in Figure 2.

Figure 1. FlexiForce Sensor A201 Model (Tekscan 2007).

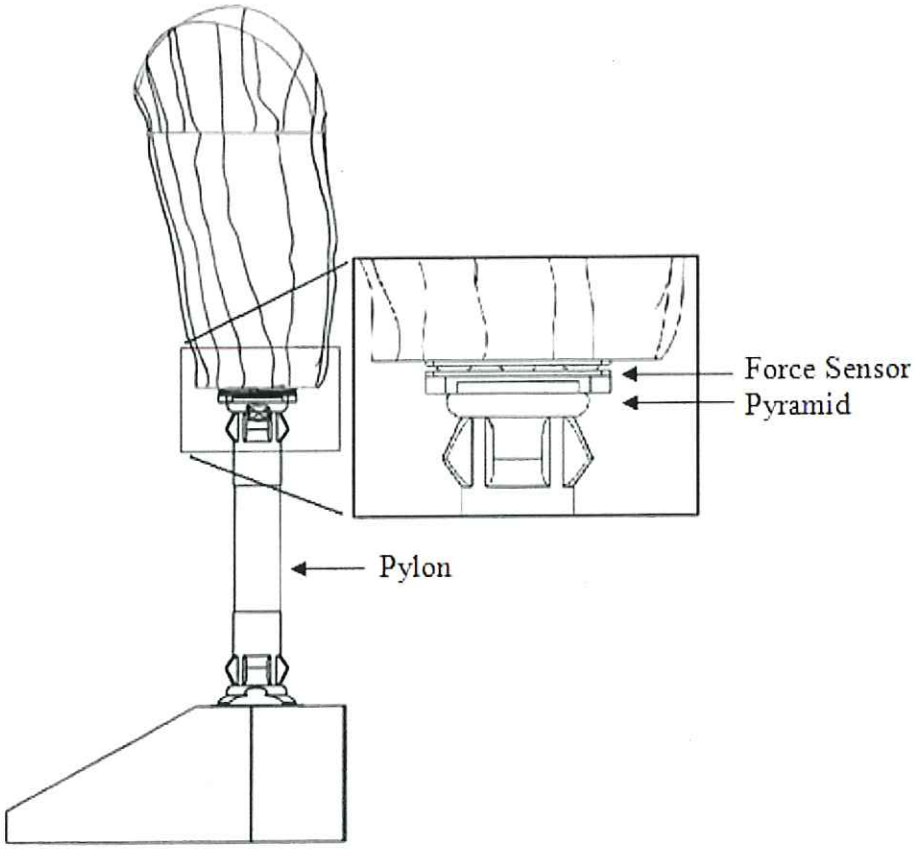

Figure 2. Force sensing device integrated into a transtibial prosthesis below the socket.

The end user of this design, a prosthetist, will be provided with a spreadsheet-type program that allows the user to input the measured resistance of each sensor. This was the basis of the data output system, which displays the force on each sensor corresponding to the respective resistance measurement, the percentage of the total force measured on each sensor and suggestions for alignment changes that may improve the force distribution on the prosthetic limb.

A computer model and simulation of the prosthesis and force sensing device was used to help verify the trends found in the results of tests conducted with the physical device. The goal was to use a ProMechanica model of the prosthesis and force sensor system to simulate the forces that can be felt in the real prosthetic limb for various alignment angles (see Section 3.4 below for more details).

3 Subsystem Designs

The design for this project can be broken down into several subsystems. The force sensor, data output, testing apparatus, and computer simulation systems will be described in further detail in the sections below.

3.1 Force Sensor System

The force sensor system is comprised of two main parts; a top and bottom half. The force sensor assembly (Figure 3) has dimensions of 2" x 2" x 0.6". The force sensor assembly is placed between the socket and pyramid and is fastened with special ordered screws seen in Figure 2. These necessary 1.5" screws are longer than those typically used to connect the pyramid to the socket because the force sensor design adds an extra 0.6 inches in between the socket and the pyramid. The screws typically used to connect the socket to the prosthesis only have to account for the small added depth of the pyramid. The two metal plates of the top and bottom halves are fabricated to match exact dimensions of the socket pyramid (2" x 2"). Ideally, the material used for these metal plates would be a titanium alloy, which is the same material used to make the socket pyramid. However, stainless steel was found to be a satisfactory substitute that would provide the necessary strength and durability material characteristics at a much lower cost.

why?

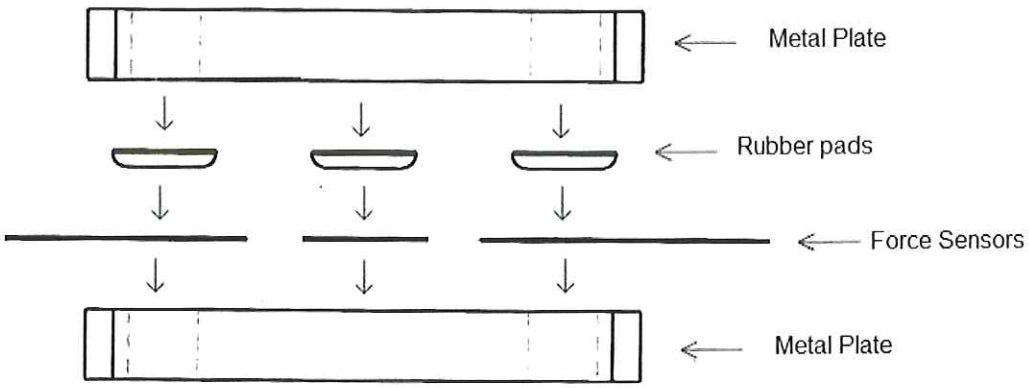

Figure 3. Exploded view of force sensor design.

The top portion of the system (Figure 4) has two components: the metal plate and the four rubber pads. The top plate has four holes cut to match those already fabricated in the pyramid. The holes in the top plate are drilled with the same size bit as the pyramid holes to ensure a tight fit between the socket and the device. In addition, the top plate has a height of 0.25 inches to help ensure this tight fit. There are four clear, dense rubber pads located under the top plate in the front-middle, back-middle, left-middle, and right-middle regions of the top plate. These placements correspond to the spots where the respective sensor is located on the bottom portion of the module. Placing the rubber pads at these regions ensures an accurate reading by concentrating the load only on the sensors. The pads were manufactured with a self-adhesive coating on the back but double-sided tape, which is non-corrosive to the rubber and stainless steel, was also applied in order to guarantee extra strong adherence. These rubber pads must stay in place because they transmit the force applied in the socket to the sensors.

Does compression of pads throw force measurement off?

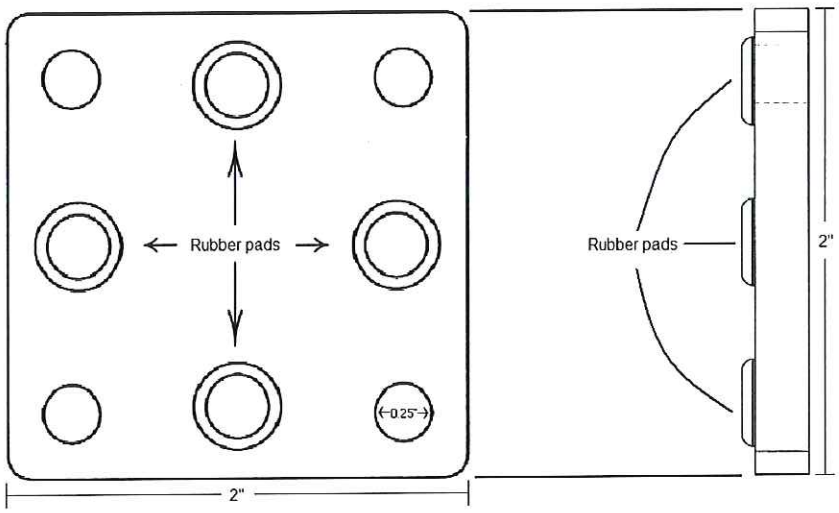

Figure 4. Top portion of force sensor design.

The bottom portion (Figure 5) is comprised of the four force sensors and the bottom metal plate. Tekscan FlexiForce, model A201 force sensors are used as the four sensors in the system. These sensors are made of two layers of polyester film, silver and a compression sensitive ink. Each force sensor was attached to the bottom plate using double-sided tape that is compatible with both the metal and the force sensor. The bottom plate has four holes drilled to be slightly bigger than the dimensions of the top plate's holes. The bottom holes are slightly larger and neither the holes in the top or the bottom are threaded to ensure that no torque will be applied through the device. As a result, the entire force is distributed through the rubber pads to be measured via the sensors and is not affected by the screw connections.

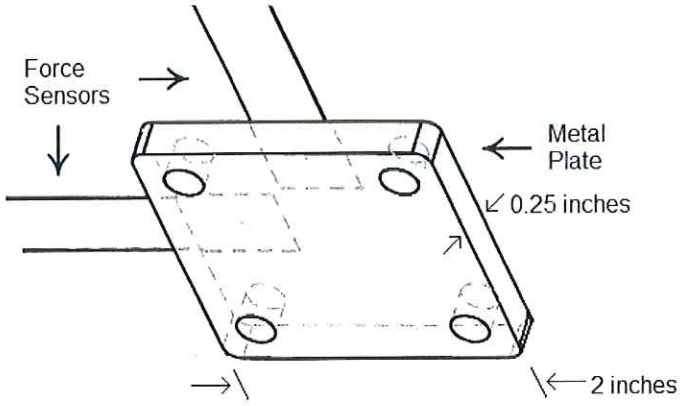

Figure 5. Bottom portion of force sensor design.

The majority of the cost of the force sensor design was in the force sensors themselves as price of the metal plates, rubber pads, and longer screws was small compared to the price of the force sensors. A 0.25" thick plate of 304 annealed stainless steel cost $7 for the two 2"x2" pre-cut plates from Westbrook Metals. A package of sixteen self-adhesive rubber pads cost a mere $2.97 at the Home Depot, leaving plenty of extras should a pad need to be replaced on the actual device. The FlexiForce force sensors had a price of $117 for a package of eight (Tekscan 2007). Since only four sensors were needed in the device, the cost of the sensors for the end user was only $58.50. The four longer screws that were necessary to ensure the safety of the prosthesis cost a total of $6.00 because they had to be special ordered. The overall cost of the force sensor module, excluding any programs or measuring devices, was $72.24.

One of the first tasks in constructing this design was to do some preliminary tests on the FlexiForce sensor to provide a proof-of-concept for the capabilities of the sensors that were selected. One force sensor was connected to a digital multimeter, which measures the resistance in the force sensor as a load is applied. An Instron machine was used to apply a compression load on the sensor. For each compressive load that was applied, a corresponding resistance value was recorded. The data collected from the experiments were then used to generate a "Force vs. Resistance" graph with a power curve fit as shown in Figure 6. These curves were necessary to interpret the output of the force sensor system using the data output system that is described later in this paper.

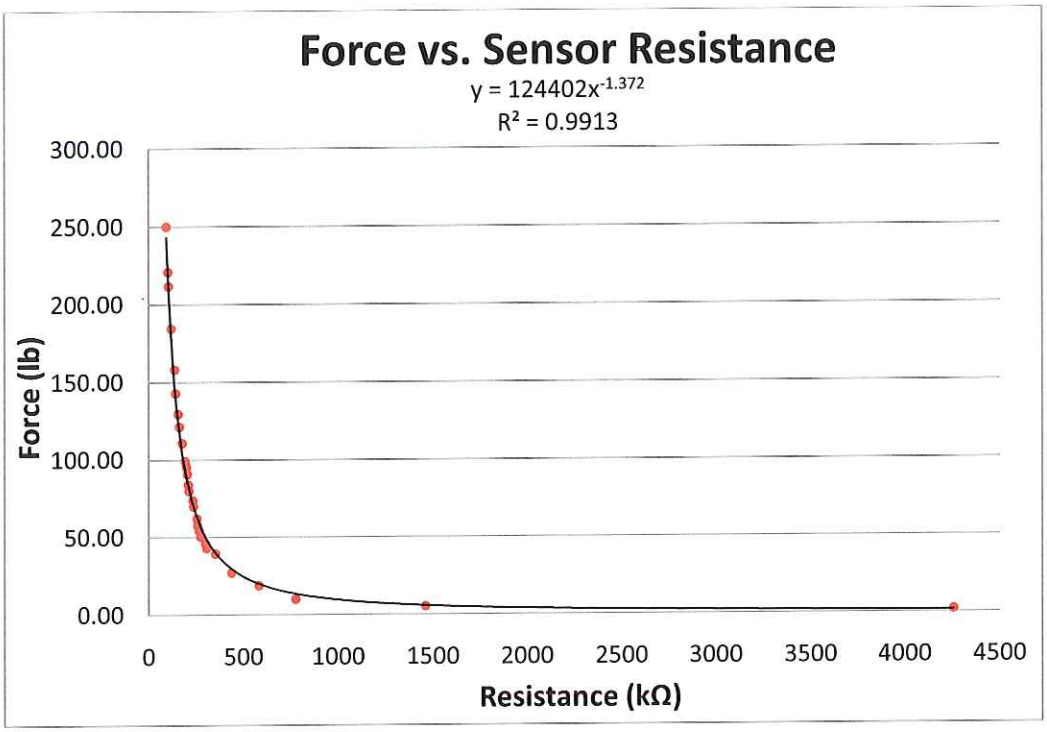

$y = \frac{1}{R}$ is linear?

Figure 6. Sensor calibration curve from preliminary measurements of force vs. resistance.

3.2 Data Output System

Tekscan provided a recommended driver circuit for the FlexiForce sensors (Figure 7), but it was not necessary to use the circuit for this project since the user will be taking static resistance measurements directly from the sensors. The data output system consists of a standard ohm meter which is connected to the sensor by the constructed leads and a spreadsheet program that takes the resistance measurements as inputs. Since these sensors are simply variable resistors, a calibration plot was generated, as described previously, for each force sensor in order to decipher the relationship between a known force and the measured resistance.

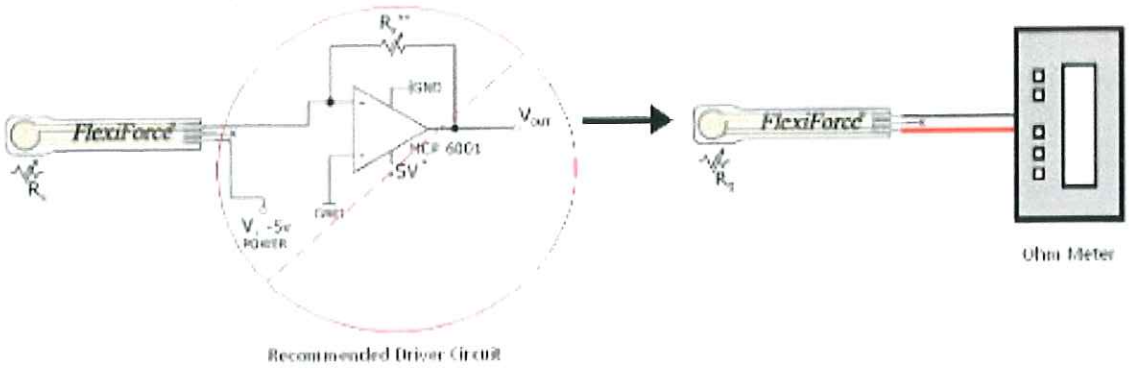

Figure 7. Obtaining output from the sensors (Image modified by J. Dizon) (Tekscan 2007).

It is important to note that the data output system was only designed to give the prosthetist a general idea of how the patient's weight is distributed along two planes. The coronal plane divides the body into anterior and posterior (front and back) sections, and the sagittal plane divides the body into left and right halves as shown in Figure 8. Therefore, the sensors provide information about the load on the prosthesis relative to the sagittal and coronal planes.

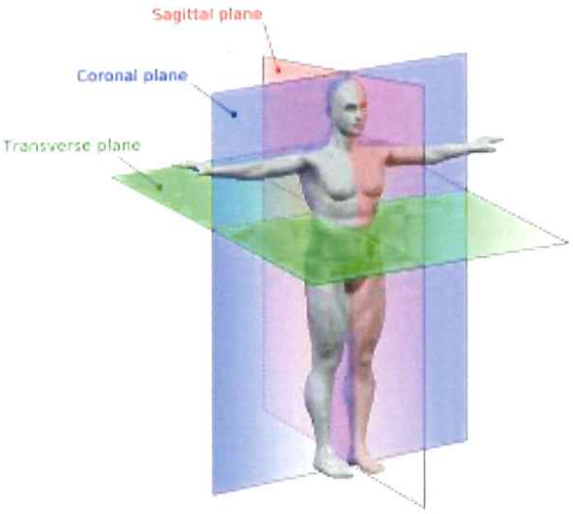

Figure 8. Planes used to describe the body and alignment (Mrabet 2008).

The prosthetist can compare the force on the outer side of the limb to the force on the inner side, and the force on the front to the force on the back. Based on the force distribution along the two planes, the spreadsheet program provides a list of suggested alignment changes that may improve the force distribution for the patient. The conditions of each individual

transtibial amputee can vary tremendously, making it practically impossible to generate one ideal curve or force distribution to fit all of the patients. The output system provides the manual method for increasing or decreasing the force on each sensor at the discretion of the prosthetist. For example, the output program lists "flex the socket" to increase the proportion of the total force on the front of the prosthesis. According to the group's technical consultant, a general system like this is actually more useful to the clinician, simply because of the inherent variability between patients. Essentially, this design provides quantitative information to supplement the qualitative description that a patient might provide based on what they feel.

With minimal background and experience in the field of prosthetics, the group could only design a product that gives suggestions to the prosthetist on how to mechanically adjust the prosthesis in order to obtain a desired weight distribution. The group assumed the clinician has access to a computer with Microsoft Excel or a similar spreadsheet program already installed. With the calibration curves for each of the four sensors and a program of equations in Excel, the prosthetist would only need to input the measured resistances read from the digital multimeter at each sensor during a static alignment fitting. The program then outputs the patient's weight distribution, in pounds, at the positions of the four sensors and provides a list of suggestions for adjustments if desired. This program was based on recommendations given by the group's technical consultant for desirable gait alignments. Appendix E provides a more detailed explanation and snapshot of the data output component of the design.

The cost of this data output portion of the overall design depended only on the price of a simple digital multimeter (which includes built-in ohm meter), since the driver circuit was not necessary and the end user was assumed to have access to a computer with a spreadsheet program. The cost of the sensors themselves fell under the force sensor subsystem as described previously. The ohmmeter should be able to measure resistances up to approximately 200 MΩ, because the sensors have infinite resistance when completely unloaded. Resistance values also go down to near 90 kΩ for a load of 250 pounds. The ohmmeter needed to have fairly good resolution and precision because at high forces (low resistances), small changes in resistance measurements resulted in comparatively large changes in force due to the power fits of the sensor calibrations curves (See Fig. 6). The Fluke 114 Electrical True RMS Digital Multimeter exceeds the needs of this system. This 550-gram multimeter is handheld and has a measurement range of 600.0 Ω to 40.00 MΩ (resolutions of 0.1 Ω and 0.01 MΩ, respectively). The accuracy is

0.9%+1 for the range up to 6 MΩ and 5%+2 for the 40 MΩ range (Fluke Corporation 2009). The Fluke 114 is listed at $129.95 by several suppliers, including Transcat, Techni-Tool and Newark. The unit includes the 9-volt alkaline battery (typical battery life is 400 hours without backlight), test leads and manual. More expensive models that have a greater variety of options and provide greater resolution or precision are also available but with a higher price tag. The choice of multimeter is at the discretion of the clinician, but it is expected that most clinicians would prefer the least expensive model that meets the needs of the design. Therefore, it was estimated that a clinician would need to spend approximately $130 for this part of the data output system. While the initial cost for this portion of the design may be relatively high, the multimeter would be used for many static alignment appointments so the cost would be very low on a per-patient basis.

4 Methods

The methods behind testing the force sensing design were divided into several steps. First, sensitivity tests were conducted on the sensors in order to verify that there was little to no deviation in the force measurements over time for a given load. Second, an immobilization apparatus was constructed to run consistent tests throughout the experiment. In the following sections, the testing procedures for both the physical and computer simulations and the process of evaluating the data collected will be explained in detail.

4.1 Sensitivity Tests

In order to determine whether or not time would be a factor in this experiment, the group conducted a series of sensitivity tests. Using the boot apparatus shown in Fig. 9 (the group's initial test apparatus design), the subject was instructed to stand still for ten seconds while data was collected from each sensor simultaneously using Labview (Fig. 10). Although these tests were performed using a different apparatus, the same force sensing component was used in testing for both the boot design and the immobilization design. The boot design was actually a more realistic and reliable representation of the data over time for this particular test because it accounts for human error.

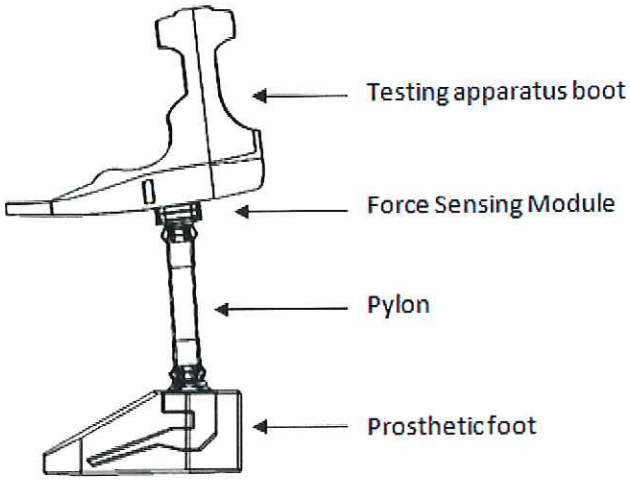

Figure 9. Boot apparatus used for sensitivity tests.

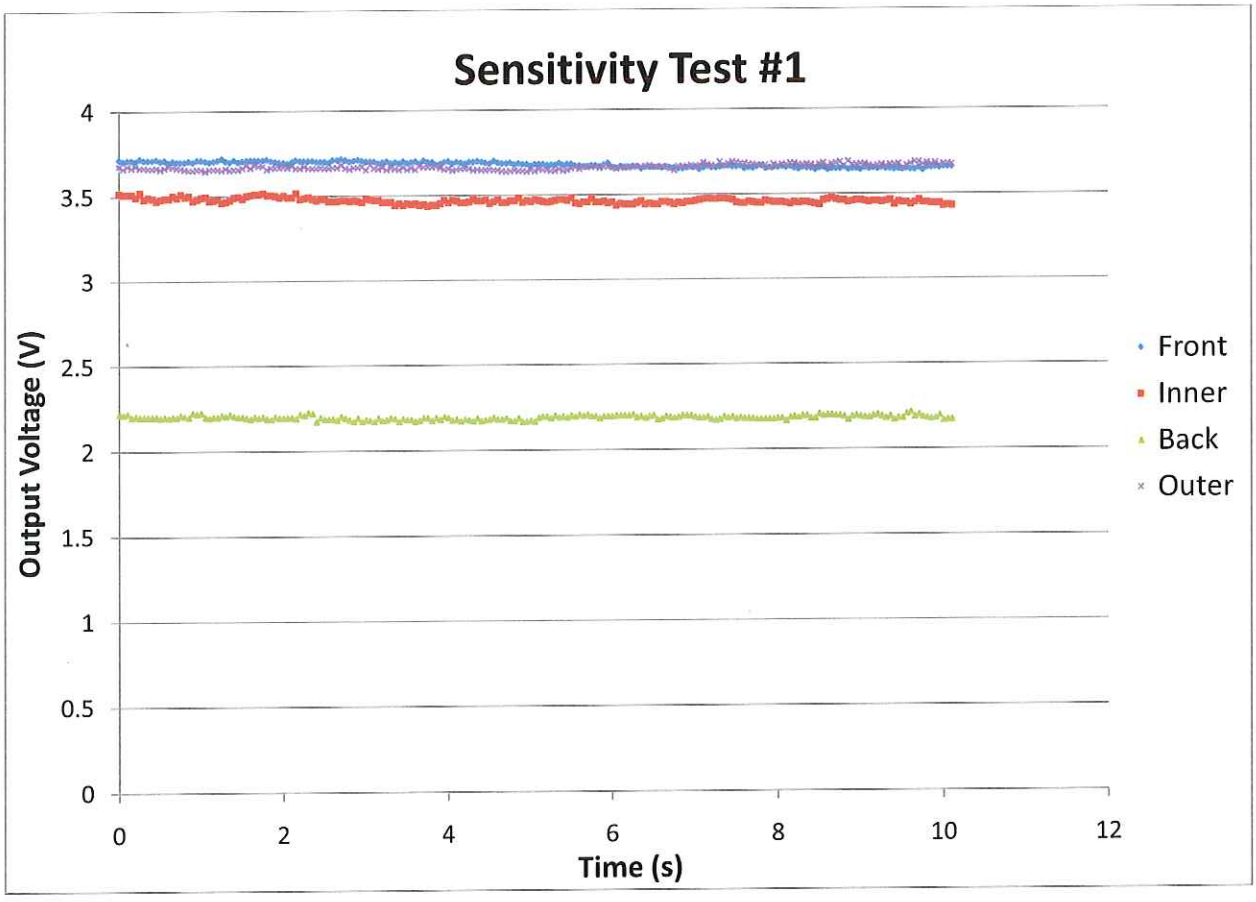

Figure 10. Example of sensitivity test data collected using Labview.

Figure 11 depicts the average force measured over 10 seconds in a sensitivity test. The voltage readings were directly related to force – a greater output voltage indicated a greater force applied to the sensor. The error bars in this plot show that the sensors' voltage output readings were fairly constant over time. This ten second sensitivity test was repeated three times with similar results each time. Figures 10 and 11 provide a good representation of all of the sensitivity test data.

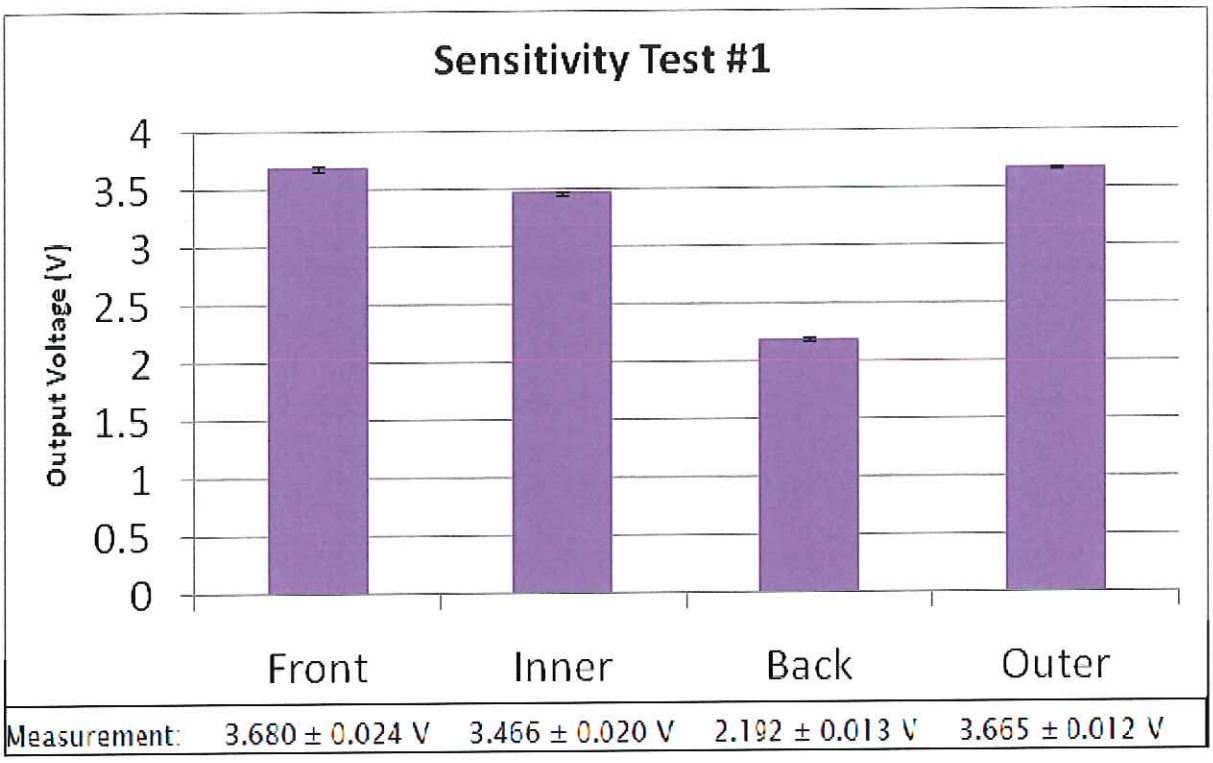

Figure 11. Average force measurements for a 10 second period in a sensitivity test.

Here, a difference in an output voltage of 0.01 V approximately corresponds to a 0.5 lb change in force. The sensitivity tests confirmed that force measurements from each of the sensors were nearly constant over time, given a steady load force. Therefore, the group was able to safely assume that the force distribution around the sensing device was constant throughout any single physical test conducted during the process and could proceed with the physical testing.

4.2 Testing Apparatus

The purpose of the designed testing apparatus was to simulate the real world application of the force measuring device without having to use actual amputees as test subjects. This helped to meet ethical and political constraints on the project while obtaining relevant physical data to test the functionality of the force measuring device and the validity of predictions made with the computer simulation. Proper measures were taken in order to guarantee the structural integrity and functionality of the testing apparatus while in use. Figure 12 depicts the immobilization test apparatus. This apparatus allowed the group to load the prosthetic limb and test the force measuring system in a stable, controlled and consistent manner without introducing the extraneous variables present in the boot testing apparatus.

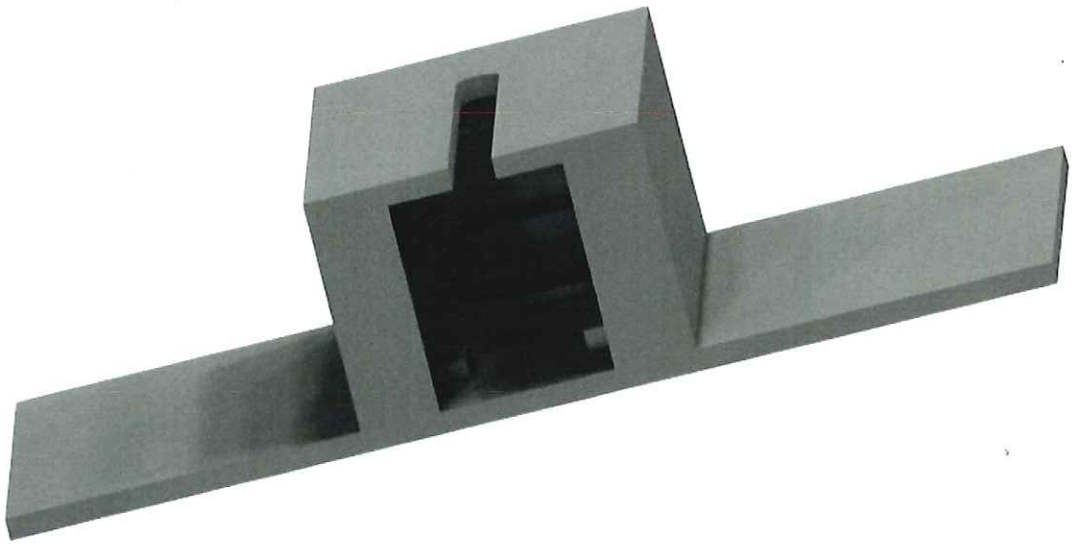

Figure 12. The immobilization test apparatus.

The basic concept of the immobilization testing device was to adapt a pole, sturdy enough to hold up to 125 lbs in place, with hardware so that it could be connected to the designed force measuring system integrated into the prosthesis. The immobilization apparatus shown in Fig. 12 was designed to hold the foot and pylon in place in order to keep the positioning consistent throughout the testing procedure. The group replaced the socket of the prosthesis with a pole attachment (Fig. 13) having a diameter small enough to fit through the

center holes of the free weights. Figure 14 depicts the entire loaded testing apparatus design used for data collection.

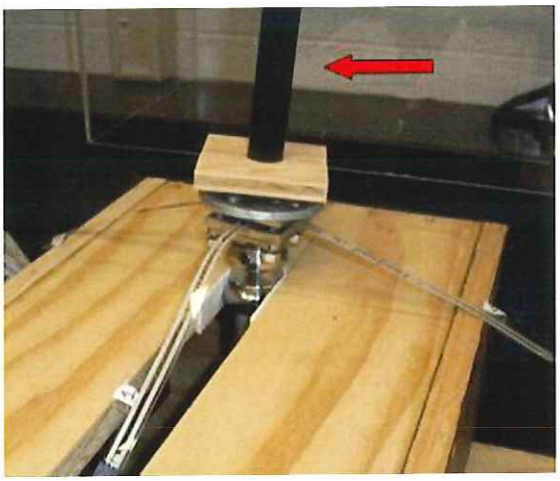

Figure 13. The prosthesis with pole attachment in place of the socket.

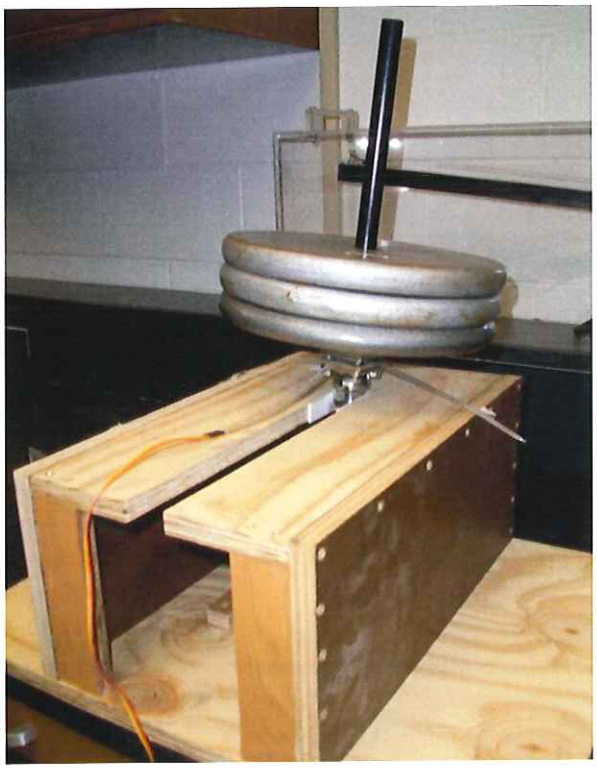

Figure 14. Loaded testing apparatus.

The immobilization apparatus restricted movement in the ankle joint and foot while still allowing the area to bear weight. This allowed the group to keep the lower leg at a specific angle with respect to the pylon just as it would with an actual amputee in the socket.

4.3 Test Matrix and Testing Procedure

The test matrix shown in Table F-1 incorporates a 3^3 factorial design of experiment. The three factors in the matrix, each tested at three levels, are weight on the prosthesis, alignment in the coronal plane, and alignment in the sagittal plane. According to the group's consultant, the range of total patient weight varies between 100 – 250 lbs. Since each leg was assumed to bear 50 percent of a patient's total weight in a static fitting procedure, the group varied the testing loads from 50 – 125 lbs in the design of experiments. Since linearity could not be assumed, three different loads of 50, 75, and 125 lbs were measured at each alignment. For each load, adjustments in the coronal and sagittal planes were executed to imitate standard clinical alignments (Fig. 8). In the sagittal plane, the pyramid at the socket was extended, set in bench, or flexed (Fig. 15). Similarly in the coronal plane, the same pyramid was adducted, set in bench, or abducted (Fig. 15). This method of testing allowed the group to measure the force distribution on the sensing device at all alignment combinations for the given load.

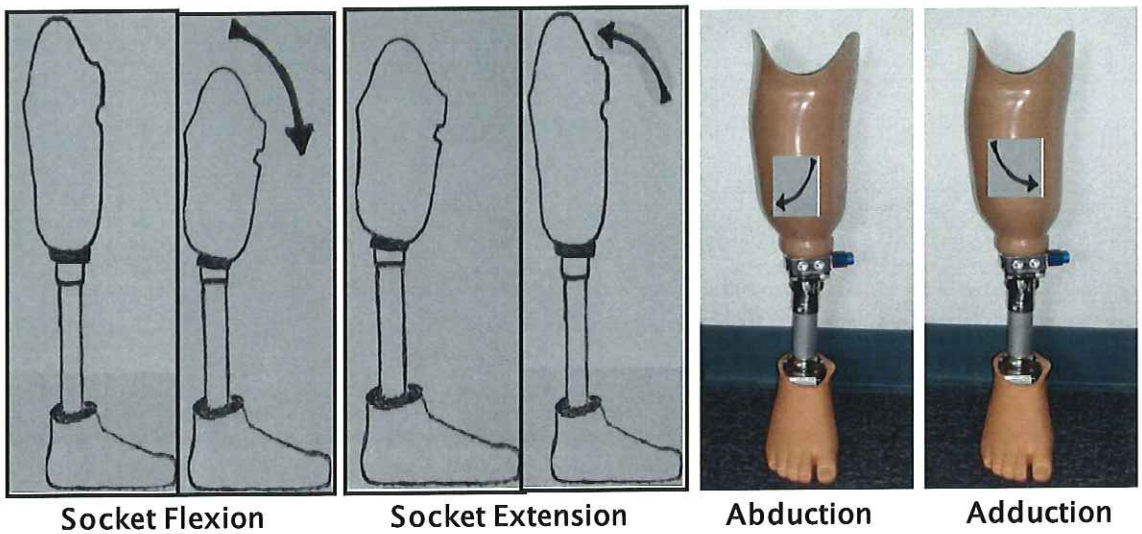

Figure 15. Direction of alignment changes at the socket used in testing.

Two replications of the factorial design of experiments (27 tests for each replication) were randomized together in order to reduce any potential bias in the testing procedure. After each test was completed, the pyramid was set back into the bench position using a standard horizontal level tool. The next test was then completed by adjusting the socket to the next assigned alignment in the randomized test matrix. Before loading the aligned apparatus for each test, an ohmmeter was used to record resistance measurements at sensors 1, 2, 3, and 4 consecutively with the unloaded prosthesis set in the immobilization apparatus. Once those measurements were recorded in the data output program, resistance measurements at the sensors were again taken with the prosthesis loaded and also recorded in the data output system. Using these data, it was possible to see if the observed trends in the output fit the trends that were expected based on the alignment, which is explained in further detail later in the report. All data were also analyzed using Minitab Statistical Software.

4.4 Computer Simulation of Prosthesis with Force Sensing Device

The computer model is a representation of a basic below-knee prosthetic leg of the sort Tiffany Forest has loaned the group. Although it was patterned on a model created by an Independent Study Project under the guidance of Dr. Peter Kelly-Zion, a significant number of features for the current model were redone to achieve compatibility with Pro/Engineer and parity with the loaner prosthetic leg. Created using Pro/Engineer, the computer simulation allows the user to adjust patient weight and socket angle in the sagittal and coronal planes. Mechanical simulations were then run based upon the desired alignment settings. The principle outputs of these simulations were the force measurements at the interfaces representing the design's force sensors. Mechanical simulations were performed with settings designated by the same factorial design matrix consisting of three variables with three levels each used for the physical testing. The full matrix design is provided in Table F-1 of Appendix F. Once the full set of tests were completed using the single-pass setting in ProMechanica, the resulting data were entered into Minitab to perform an ANOVA analysis and generate coefficients for prediction equations.

4.5 Minitab

Minitab was used to analyze the experimental data generated both in the physical tests as well as the ProMechanica simulations. The original intent was for a limited number of physical tests to be conducted under the assumption that the computer simulations could be run with little supervision to generate all the data necessary to produce statistically meaningful prediction equations through Minitab. These equations would then be used to cross-validate the physical results and thereby provide an accurate model of the physical system quickly and efficiently. Through the course of conducting the test runs, it became clear that results from the physical system and computer simulation did not agree in terms of the absolute magnitude of the forces measured. Therefore, the focus on the comparison between the physical and computer simulations shifted to comparing the qualitative force distribution trends between the two. Main effect plots were produced in Minitab to compare the data based on this information. Within the respective data sets, an ANOVA analysis was run to test the statistical significance of the data and produce prediction equations using a Design of Experiments method. The coefficients for the appropriate variables to include in the prediction equation were chosen based on their p-values which showed whether or not they were statistically significant. The validity of the prediction equations was assessed by checking to see if they could correctly predict the force measurements for a test that had already been run.

5 Results

To test the final design, we used the immobilizing testing apparatus described in Section 4.2. Force measurements for each alignment were taken twice to check for repeatability and enable us to perform statistical analyses with our data. In general, we observed that the average force measured by each sensor for each alignment satisfies the trends that were expected. However, the magnitude of the physical force measurements varied widely. The trends in the forces measured using the computer model match the physical data trends in both the coronal plane (side to side) and the sagittal plane (front to back).

5.1 Physical Testing Results

Overall, the physical tests were not repeatable. When the same alignment was tested twice (using a randomized testing order), the two measurements differed by as much as 28 pounds or as little as 0.025 pounds. These extremes were both found on a single sensor, the "outer" sensor, but similar variations were present for the other sensors as well. While the lack of repeatability was discouraging, the relative force distributions satisfied the trends we expected based on information provided by our technical consultant. For example, when the socket was extended, we expected to see more force on the back sensor than on the front. When the socket was flexed, we expected to see the opposite. The average values conformed to this trend as shown in the "Main Effect" plots generated by Minitab (Figs. G-1 and G-2). The average values in the coronal plane also conformed to the anticipated trends (Figs. G-3 and G-4).

When the physical test data was analyzed using Minitab Statistical Software, we discovered that prediction equations cannot be acquired for variables with three levels. We did, however, run an Analysis of Variance (ANOVA) test using all of the data and generate the Main Effect plots referenced above. The Main Effect plots using three levels for each variable showed that the relationships were not perfectly linear, but they were reasonably close to linear. The ANOVA analysis (see Appendix H for all ANOVA results) provided R-squared values for each sensor, which indicated how well a linear regression fit the data. The lowest R-squared value was 88.57% and the highest R-squared value was 94.84%. For our purposes, these R-squared values were high enough to justify excluding the center point data in a second Minitab analysis so that prediction equations could be determined using linear regression.

In order to obtain prediction equations for our physical design, we removed the middle level (75 pound-level from weight and "bench" from sagittal and coronal angle) and used only two levels for each variable. The Main Effect plots generated using two levels with two replications each closely matched those using three levels and continued to agree with the expected trends (Figs. G-5 to G-8). Once again, the ANOVA analysis returned high R-squared values (lowest was 95.10%) indicating that Minitab's linear regression was appropriate for these data. The prediction equations generated in the two-level analysis are of the general form shown by Eq. 1:

$$Force = c_0 + c_1 * Weight + c_2 * Sagittal + c_3 * Coronal + c_4 * Weight * Sagittal +$$

$$c_5 * Weight * Coronal + c_6 * Sagittal * Coronal + c_7 * Weight * Sagittal * Coronal \quad \text{Eq. 1}$$

The p-values provided by the ANOVA analysis indicated which of these terms have a significant impact on the force measurement that was unlikely to be due to chance. We observed that the weight term and the constant were significant terms in the prediction equations for all four sensors ($p < 0.001$). The significance of other terms was dependent on the sensor's location (sagittal plane or coronal plane). For the sensors in the sagittal plane ("front" and "back"), the p-values indicated that the sagittal and weight*sagittal terms were significant ($p < 0.001$), while the remaining terms, all of which include the coronal factor, were relatively insignificant. Although the p-values for the terms involving the coronal factor were less than the traditional threshold value of 0.05, they were at least 3 times larger than the p-values for the weight and sagittal terms. For the sensors in the coronal plane ("inner" and outer"), we saw that the coronal and weight*coronal terms were significant ($p < 0.001$), while the terms involving the sagittal factor were insignificant with p-values greater than 0.08. The prediction equations for the physical data were then reduced to the following forms where "sagittal" is equal to -1 for extending the socket or +1 for flexing the socket (Eq. 2), and "coronal" is equal to -1 for adducting the socket or +1 for abducting the socket (Eq. 3):

$$F_{sagittal\ sensor} = c_0 + c_1 * Weight + c_2 * Sagittal + c_3 * Weight * Sagittal \quad \text{Eq. 2}$$

$$F_{coronal\ sensor} = c_0 + c_1 * Weight + c_2 * Coronal + c_3 * Weight * Coronal \quad \text{Eq. 3}$$

Table 1 provides the values for the coefficients in the prediction equation for each force sensor. When we evaluated the ability of these equations to predict the forces measured by our physical force-sensing device (see data in Table I-1), we discovered that for the physical data,

these equations have certain limitations. One limitation was that the equations (Eq. 2 and 3) were less successful than the computer simulation equations in predicting the force measurements for the midpoint tests that were excluded in this Minitab analysis, such as tests where the total load on the prosthesis was 75 pounds. Another issue was that, since the repeatability of the sensor measurements was poor, the equations predict an average measurement rather than matching either repetition exactly. This limitation was due more to the sensor's fluctuation than the linear regression analysis performed by Minitab. Despite the limitations of the model, we saw the same trends in the force distribution in the predicted values as we expected based on an understanding of the physical system.

Table 1. Prediction Equation Coefficients for Physical Test Data.

	Sagittal Plane Sensors		Coronal Plane Sensors	
Coefficient	Front Sensor	Back Sensor	Inner Sensor	Outer Sensor
c_0	2.30237	-2.28196	2.65392	3.35579
c_1	0.200375	0.189827	0.120992	0.182157
c_2	-7.53004	4.24762	-5.21958	3.23113
c_3	0.236098	-0.140920	0.142312	-0.153480

5.2 Computer Simulation Results

Repeatability was not an issue with the computer simulation of our design because ProMechanica will load the model in the exact same way every time if the alignment is defined the same way. Therefore, the test matrix was only performed once in ProMechanica. A randomized testing order was also unnecessary for the computer simulation, because a previous test does not affect the current test.

When the computer simulation data was analyzed in Minitab, we still entered two runs for each test in order to match the procedure used to analyze the physical testing data. However, for this analysis, the two values for each test were identical. Using three levels for each variable, we could only obtain effects plots (Figs. G-9 to G-12) and ANOVA analyses (Appendix H) for each sensor as we did when analyzing the physical test data. The negative values occurring in our computer simulation were the result of ProMechanica's ability to measure tension in addition

to compression. In order to obtain prediction equations for the force sensors in the computer simulation, we again removed the center or "bench" level for each variable so that Minitab could perform linear regression with our data. The Main Effect plots for sensors 2 (inner) and 4 (outer) were very consistent between the 3-level and 2-level Minitab analyses because the data for sensors in the coronal plane was linear even with the center data points included (see Figs. G-15 and G-16). The data for sensors in the sagittal plane (front and back sensors) was also very linear as the socket angle was varied from extended to flexed (Figs. G-13 and G-14). Since all of the ProMechanica data was highly linear, the prediction equations generated by the 2-level Minitab analysis were able to approximate the force measurements on all four sensors to within 1 pound of the ProMechanica simulation values (including bench values) as shown in the data provided in Appendix I, Table I-2.

There were no p-values or other indications of statistical significance for the Minitab analysis of the ProMechanica data since there was no variation between tests. We decided to reduce the prediction equations generated with the computer simulation data to include only the terms that were significant for the physical testing (See Eq. 2 and 3). This decision was based on an understanding of the physical system for different alignment and loading scenarios. Table 2 below contains the coefficient values for these prediction equations.

Table 2. Prediction Equation Coefficients for ProMechanica Test Data.

	Sagittal Plane Sensors		Coronal Plane Sensors	
Coefficient	Front Sensor	Back Sensor	Inner Sensor	Outer Sensor
c_0	8.3333E-6	1.7764E-15	2.6667E-5	8.2500E-7
c_1	0.590633	-0.0909828	0.259900	0.240677
c_2	8.3333E-6	-7.1054E-15	2.6667E-5	-8.4167E-7
c_3	0.234049	-0.234747	0.234601	-0.234404

5.3 Comparison of Physical Design and Simulation

Using three levels for each variable to generate Main Effect plots, we saw that the physical testing and the computer simulation agree (trend-wise) for sensors 2 (inner) and 4

(outer). Based on these data, we saw that the computer simulation was acceptable in qualitatively predicting the relative force distribution in the coronal plane, but the magnitude of the force measured by the physical sensor did not match the magnitude determined by the simulation (see Appendices G and I). The Main Effect plots matched trend-wise but again not in magnitude when we compared the physical testing and computer simulation data for sensors 1 (front) and 3 (back). The discrepancies in the sagittal plane measurements were the result of the inability of our sensors to measure tension. The ProMechanica simulation was able to collect negative (tension) and positive (compression) force measurements, while our sensors could only measure compression. Therefore, it was especially difficult to assess the validity of the computer simulation as a model for the physical device in the sagittal plane. Since the physical testing data agreed with the expected *trends* in both the coronal and sagittal planes, we believe that our force measuring design is validated to an extent even though it does not produce the force magnitudes predicted by the computer simulation. Based on the analysis of both the physical and computer simulation test results, we have identified several limitations of our device in its current state. These limitations will be discussed in the following section.

6 Conclusions and Recommendations

The objective of this project was to design and develop a prototype device to provide quantitative measurements of the force distribution on a transtibial prosthesis during a static alignment procedure. Our objectives also included using these measurements to make clinically relevant recommendations for alignment changes that should improve the fit of the prosthesis for an amputee, and using a computer simulation to model the physical system and collect additional data. In general, our goal was to provide a more scientific and cost effective procedure for fitting the prosthesis in comparison to current observational gait analysis and computer gait analysis methods, respectively. We believe our project was successful in meeting these objectives and goals. Using both the computer simulation and the physical prototype, we were able to obtain information about the trends relating force distribution and prosthetic alignment. Using the trends observed in the data, we were able to follow through on our plan to provide suggested alignment changes in a data output program to change the force distribution qualitatively. These trends were verified by our technical consultant Ms. Tiffany Forest, MSPO.

Due to the limitations of the sensors used in the physical prototype, we were not able to obtain good quantitative information that could be used to provide exact alignment change suggestions to produce a specific numerical change in the force measurement. The FlexiForce sensors used in the prototype had poor repeatability and were inaccurate over time since they failed to maintain parity with the initial calibrations. They were also unable to measure tension, which caused irresolvable discrepancies between the physical tests and the computer simulation. It was also discovered that these sensors exhibited very non-linear behavior in ranges of interest, introducing extra uncertainty where a small error in the resistance reading resulted in a large error in the force measurement in the upper range of the weights applied. The time constraint on this project was also a limiting factor in the development of correlations between alignments and force measurements. In order to obtain more reliable correlations, we would have needed to run our design of experiments for at least ten to fifteen replications. Our time constraint did not allow us to repeat the experimental measurements with a new set of sensors and a large number of replications.

Our recommendations toward improving the design include implementing more accurate force transducers. We recommend that the new sensors have more linear behavior in the weight range appropriate for a transtibial force sensing device, in contrast to the extremely non-linear relationship between force and resistance for the FlexiForce sensors we used, as shown in Fig. 6 previously. In addition these new sensors would need to have the ability to measure not only compression but tension as well. Using a sensor that measures tension would allow the force measurements from the physical tests to more accurately mirror those of the computer simulations which take tension forces into account. An example of this type of sensor would be a strain gage. The resistance of strain gages is directly related to the strain imposed on them as long as the gage material is not stressed past the linear elastic region, which can be avoided through proper load cell design. This relationship holds for both compression (negative) and tension (positive) strain. We believe that with more effective sensors and a large number of test replications, the data collected with the physical system could be used to develop more exact indications for the alignment changes that would produce a specific force distribution. We also anticipate that if more accurate force sensors are used in the sensing module, the computer model could be more useful for cross-validation between the actual alignments and the simulations.

7 Bibliography

Boone, David, CP, MPH, PhD. "The Next Challenge in Prosthetics." (Rehab Management) July 2009.

Fluke Corporation. *Fluke 114 Electrical Multimeter.* 2009. http://us.fluke.com/usen/Products/Fluke+114.htm?catalog_name=FlukeUnitedStates&category=IND(FlukeProducts) (accessed November 2009).

—. *Fluke 77 IV Series Digital Multimeter.* 2009. http://us.fluke.com/usen/Products/Fluke+77+IV.htm?catalog_name=FlukeUnitedStates&category=HMA(FlukeProducts) (accessed November 2009).

Mrabet, Yassine. *Human Anatomy Planes (Image).* June 7, 2008. http://en.wikipedia.org/wiki/File:Human_anatomy_planes.svg (accessed with permission to use under CC-BY-SA).

OnlineMetals.com. *Stainless HRAP Plate 304 Annealed.* 2009. http://www.onlinemetals.com/merchant.cfm?pid=724&step=4&showunits=inches&id=233&top_cat=1 (accessed November 2009).

Orthocare Innovations. *Smart Pyramid.* 2009. http://www.orthocareinnovations.com/category.php?cat=1029 (accessed October 2009).

Sanders, Joan E, PhD, Robert A., MSME Miller, David N., BSME Berglund, and Santosh G., PhD Zachariah. "A modular six-directional force sensor for prosthetic assessment: A technical note." *Journal of Rehabilitation Research and Development* 34, no. 2 (April 1997): 195-202.

Tekscan. *FlexiForce Force Sensors.* 2007. http://www.tekscan.com/flexiforce/flexiforce.html (accessed October 2009).

The Widget MFG, Co., Inc. *Rubber Stoppers.* 2009. http://www.widgetco.com/00-rubber-stoppers-plugs (accessed November 2009).

University of Chicago Press Staff. *The Chicago Manual of Style.* 15th rev. Chicago, IL: University of Chicago Press, 2003.

A Final Budget

Date Submitted: 4/13/2010
Submitted By: Alexandra Leamy
Group Name: GAIT
Advisor Name: Mahbub Uddin

Income

Date	Sponsor	Description	Budgeted Amount	Actual Amount
9/2/2008	Engr Dept	Seed Money	$1,200	$1,200
10/28/2009	Michael Brothers	CAM Walker	$90.00	$90.00
Total Income				$1,290

Expenses

						Status (Check one)			
Date	Vendor	PO #	Item Description	Status (Planned/ Pending/ Cleared)	Budgeted Amount	Actual Amount	Internal	Dept Purchase Order	PCARD	Reimburse-ment
10/20/2009	Tekscan		A201 Force Sensor	Cleared	$150.00	$132.00		x		
10/28/2009	Michael Brothers		CAM Walker	Cleared	$90.00	$90.00	x			
12/3/2009	Engr Dept		Op Amps (x4)	Cleared	$1.08	$1.08	x			
1/22/2010	Home Depot		Metric #12.9 screws	Cleared	$4.00	$2.80				x
1/14/2010	Westbrook Metals	3183426	Stainless Steel cut plates (2"x2" (2), 2"x4" (2))	Cleared	$100.00	$17.00		x		
1/19/2010	Home Depot		Vinyl & Rubber Pads	Cleared	$4.66	$3.93				x
1/28/2010	Ace Bolt & Screw		Assorted bolts & nuts	Cleared		$15.72				x
2/4/2010	HEB		Double Sided Tape	Cleared		$4.08				x
2/23/2010	Bed Bath and Beyond		Precision Digital Scale	Cleared		$54.05				x
3/8/2010	Central Market		Testing Food	Cleared		$63.91				x
3/22/2010	Academy Sports		(3) 25 lbs weights	Cleared		$68.93				x
3/17/2010	Walmart		Sponge Tape	Cleared		$2.49				x
4/27/2010	Jenny's Priniting (Trinity)		Printing & Binding of Final Report X2 (Dr. N & Dr. Uddin)	Pending	$19.98	$0***	x			
Total Expenses					**$350**	**$455.99**				

Budget Remaining	**$834.01**

*** Does not come out of project budget prior to submission - will be charged to the department.

Figure A- 1. Final Budget.

B Bill of Materials and List of Vendors

The bill of materials (Table B-1) is intended to provide an analysis of the cost associated with assembling one force sensing module and its output system that a prosthetist could integrate into a prosthetic limb.

Table B-1. Bill of Materials and Vendors for one design unit.

Item	Vendor	Amount Required	Cost/ Unit	Total Cost
2" x 2" 304 Annealed Stainless Steel Plates	Westbrook Metal, Inc.	2	$3.50	$7.00
Rubber Pads	Home Depot	4	$0.19	$0.74
FlexiForce Model A210-100 Sensors	Tekscan, Inc	4	$14.63	$58.50
Custom Ordered 3" metric screws	Ace Bolt & Screw	4	$1.50	$6.00
Fluke 114 Digital Multimeter	Fluke Corporation (Through Transcat, Techni-Tool or Newark)	1	$129.95	$129.95
Total Cost				**$202.19**

C Final Work Breakdown Structure and Schedule

GAIT Gantt Chart with WBS Codes

ID	WBS Code	Task Name	Start	Finish
1	1.3.3.1	Construct Force Sensor Module	Thu 1/14/10	Thu 2/4/10
2	1.3.3.2	Construct Testing Apparatus	Thu 1/14/10	Thu 2/4/10
3	1.3.3.3	Construct Data Output System Spreadsheet w/o Alignment Changes	Thu 1/14/10	Thu 2/4/10
4	1.3.4.2.1	Calibration Curves for Sensors	Thu 1/14/10	Tue 1/19/10
5	1.3.4.2.2	Construct Labview VI for POC	Thu 1/14/10	Thu 1/28/10
6	3.3	Poster Submissions	Tue 1/26/10	Tue 2/2/10
7	1.3.4.2.3	Labview Tests of Sensors using Apparatus	Thu 2/4/10	Tue 2/9/10
8	1.3.5.2	P/POC Presentation Practice (Internal)	Thu 2/4/10	Thu 2/11/10
9	1.3.5.1	P/POC Demonstration	Thu 2/4/10	Thu 2/18/10
10	1.3.4.1	Pro-Mechanica Simulation	Tue 2/9/10	Thu 3/4/10
11	1.4.4.3	Actual Prosthesis Testing/ Compare Results to Minitab	Thu 2/25/10	Wed 3/24/10
12	1.4.4.2	Minitab Modeling	Thu 3/4/10	Fri 3/26/10
13	1.4.3.1	Construct Data Output System With Alignment Change Suggestions	Sat 3/13/10	Sun 4/18/10
14	1.4.3.2	Construct New Testing Apparatus (not boot)	Tue 3/16/10	Thu 3/18/10
15	2.1.3	Reimbursement Request	Tue 3/30/10	Thu 4/1/10
16	1.4.5.3	Final Project Report Draft	Thu 4/1/10	Thu 4/15/10
17	1.4.5.1	Bill of Materials	Tue 4/6/10	Thu 4/15/10
18	1.4.5.2	CAD Drawings	Tue 4/6/10	Thu 4/15/10
19	1.4.5.4	Final Project Presentation Practice	Wed 4/14/10	Tue 4/20/10
20	1.4.5.4	Final Project Presentation	Wed 4/14/10	Thu 4/22/10
21	1.4.5.3	Final Project Report	Thu 4/8/10	Tue 4/27/10
22	2.5	Executive Summary	Sun 4/25/10	Tue 4/27/10
23	1.5.1	Cleanup of Area/ Project	Tue 4/27/10	Fri 4/30/10

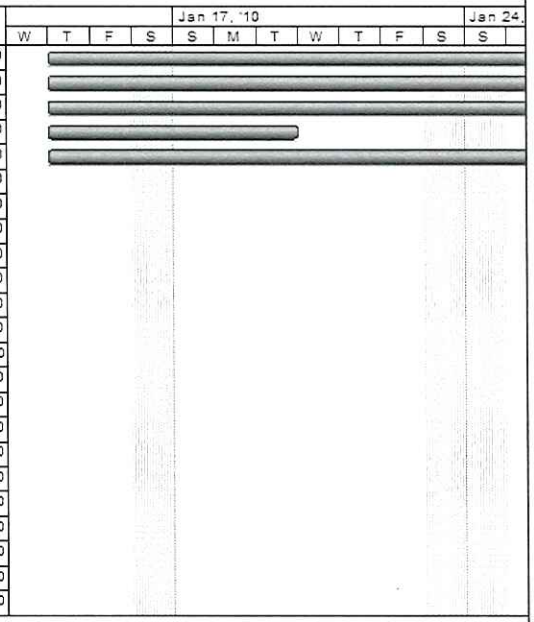

Project: Gantt Chart
Date: Tue 4/13/10

Task — Milestone — External Tasks
Split — Summary — External Milestone
Progress — Project Summary — Deadline

Page 1

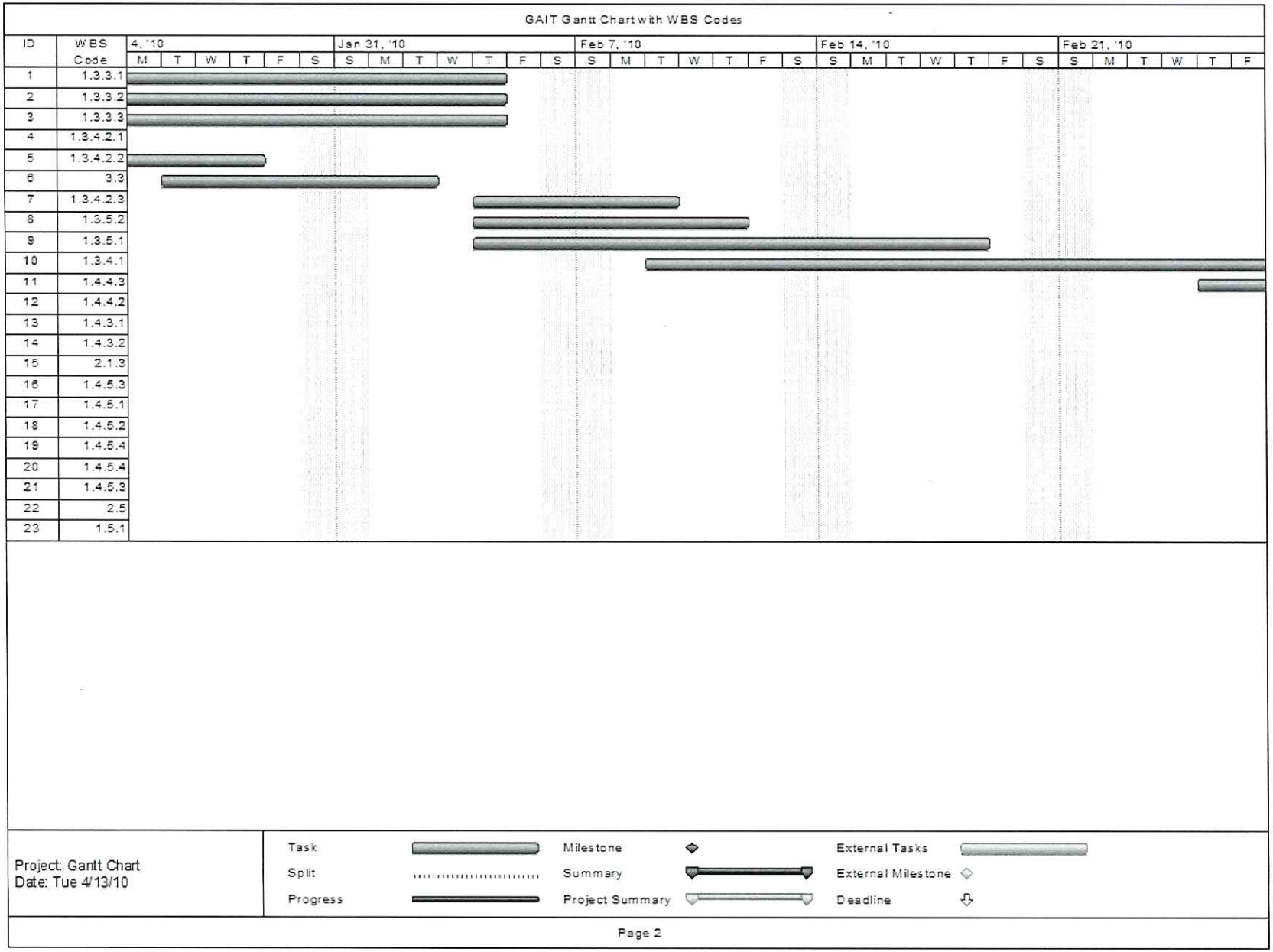
GAIT Gantt Chart with WBS Codes
ID
WBS Code
4, '10
Jan 31, '10
Feb 7, '10
Feb 14, '10
Feb 21, '10
M T W T F S S M T W T F S S M T W T F S S M T W T F S S M T W T F
1 1.3.3.1
2 1.3.3.2
3 1.3.3.3
4 1.3.4.2.1
5 1.3.4.2.2
6 3.3
7 1.3.4.2.3
8 1.3.5.2
9 1.3.5.1
10 1.3.4.1
11 1.4.4.3
12 1.4.4.2
13 1.4.3.1
14 1.4.3.2
15 2.1.3
16 1.4.5.3
17 1.4.5.1
18 1.4.5.2
19 1.4.5.4
20 1.4.5.4
21 1.4.5.3
22 2.5
23 1.5.1
Project: Gantt Chart
Date: Tue 4/13/10
Task
Split
Progress
Milestone
Summary
Project Summary
External Tasks
External Milestone
Deadline
Page 2

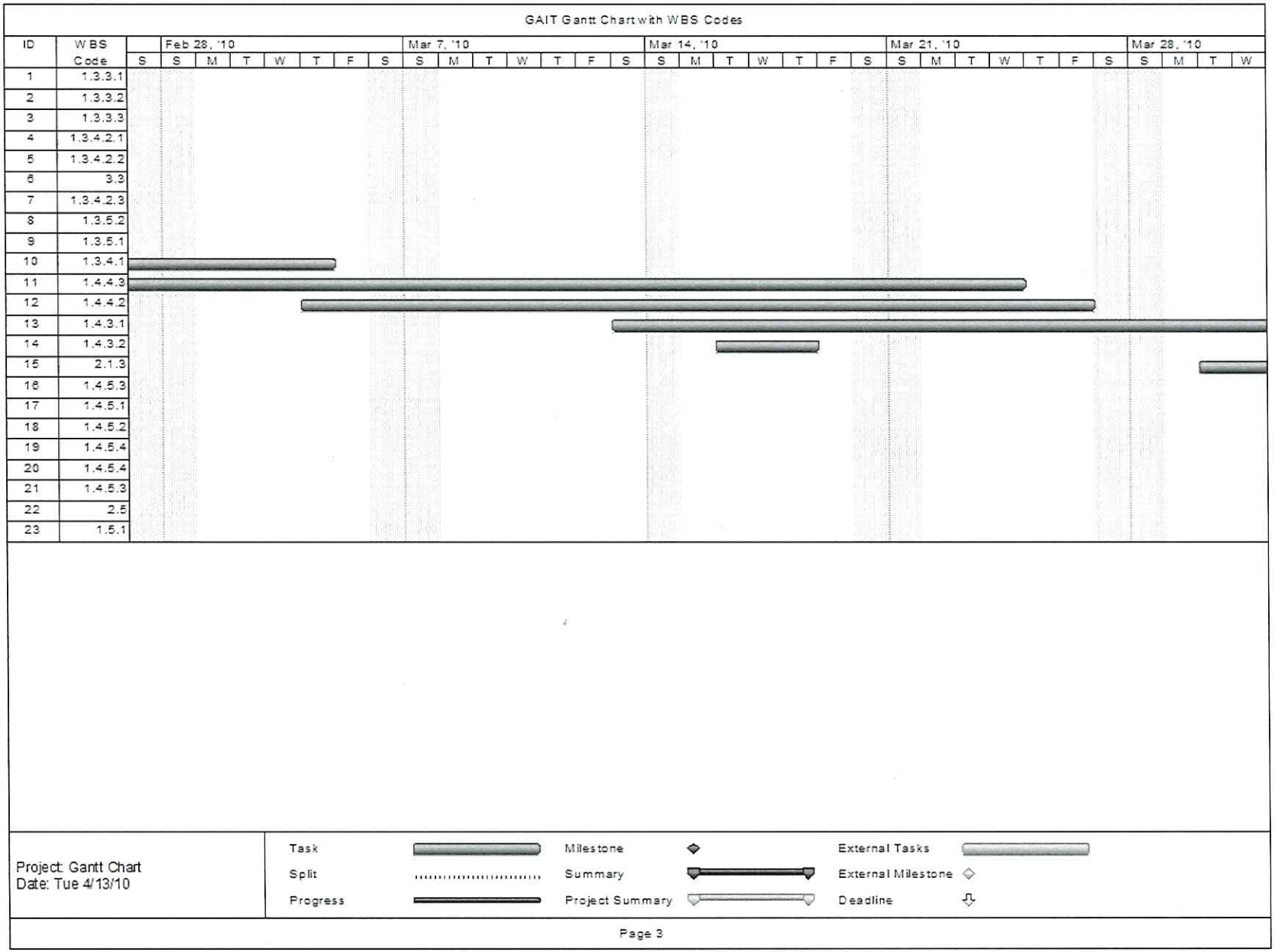
GAIT Gantt Chart with WBS Codes
ID
WBS Code
Feb 28, '10
Mar 7, '10
Mar 14, '10
Mar 21, '10
Mar 28, '10
S S M T W T F S S M T W T F S S M T W T F S S M T W T F S S M T W
1 1.3.3.1
2 1.3.3.2
3 1.3.3.3
4 1.3.4.2.1
5 1.3.4.2.2
6 3.3
7 1.3.4.2.3
8 1.3.5.2
9 1.3.5.1
10 1.3.4.1
11 1.4.4.3
12 1.4.4.2
13 1.4.3.1
14 1.4.3.2
15 2.1.3
16 1.4.5.3
17 1.4.5.1
18 1.4.5.2
19 1.4.5.4
20 1.4.5.4
21 1.4.5.3
22 2.5
23 1.5.1
Project: Gantt Chart
Date: Tue 4/13/10
Task
Split
Progress
Milestone
Summary
Project Summary
External Tasks
External Milestone
Deadline
Page 3

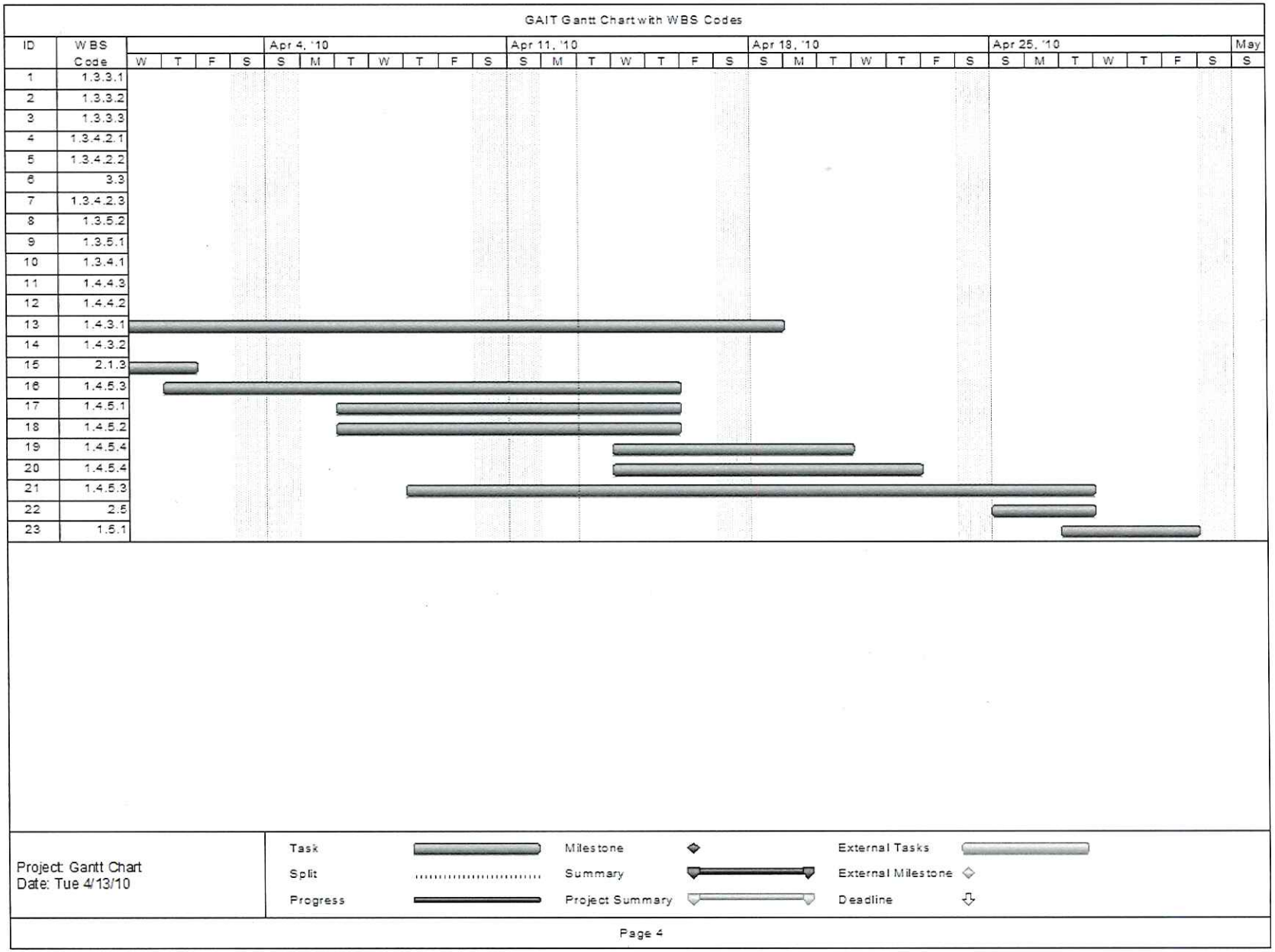
GAIT Gantt Chart with WBS Codes
ID
WBS Code
Apr 4, '10
Apr 11, '10
Apr 18, '10
Apr 25, '10
May
W T F S S M T W T F S S M T W T F S S M T W T F S S M T W T F S S
1 1.3.3.1
2 1.3.3.2
3 1.3.3.3
4 1.3.4.2.1
5 1.3.4.2.2
6 3.3
7 1.3.4.2.3
8 1.3.5.2
9 1.3.5.1
10 1.3.4.1
11 1.4.4.3
12 1.4.4.2
13 1.4.3.1
14 1.4.3.2
15 2.1.3
16 1.4.5.3
17 1.4.5.1
18 1.4.5.2
19 1.4.5.4
20 1.4.5.4
21 1.4.5.3
22 2.5
23 1.5.1
Project: Gantt Chart
Date: Tue 4/13/10
Task
Split
Progress
Milestone
Summary
Project Summary
External Tasks
External Milestone
Deadline
Page 4

D ProEngineer Drawings

The force sensor prototype will be incorporated into the prosthesis between the socket and the pyramid that connects the socket to the pylon as shown below. It will be necessary to replace the standard screws with long, customized screws to accommodate the new component's thickness.

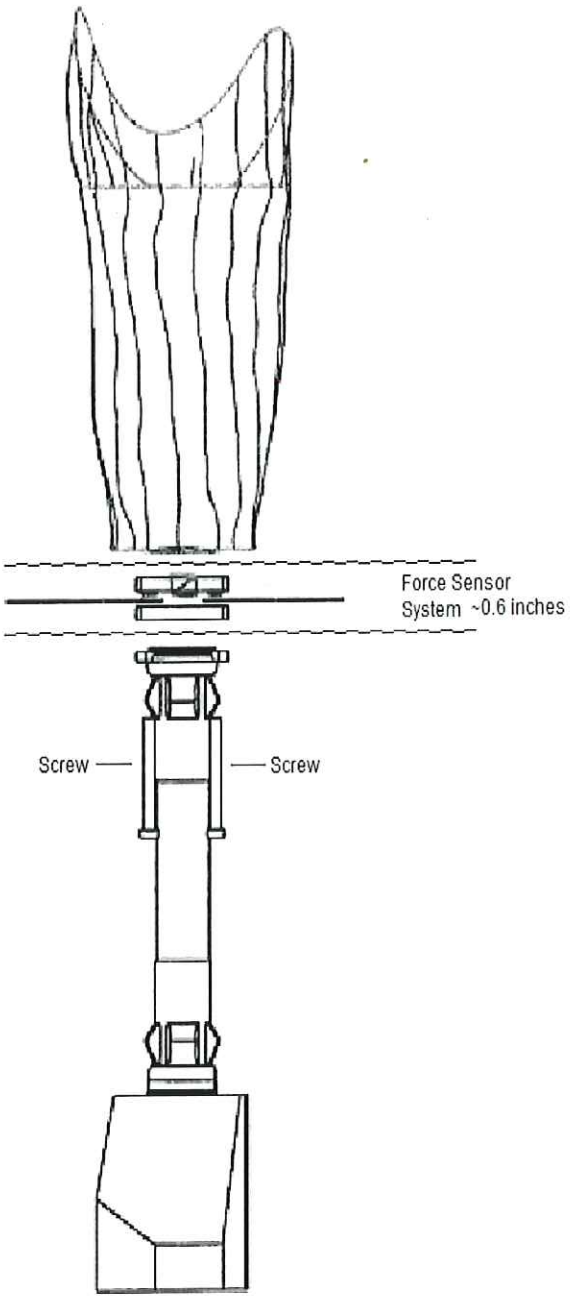

Figure D-1. Enlarged image of the prosthesis with the force sensor prototype incorporated.

E Software

The software portion of this design consists of a spreadsheet program that meets several specifications. The input to the program, given by the clinician, is the resistance measured by each sensor while the patient is in midstance. When static measurements are being taken (rather than dynamic, or walking measurements), "midstance" refers to putting half of the body weight on the prosthetic limb. The program takes the resistance values and displays forces in pounds using the calibration equations generated for each sensor. The program provides recommendation for alignment changes that should reduce or increase the force on a given sensor area. The force distribution information should also provide an experienced prosthetist with the quantitative information they need to make decisions regarding prosthetic alignment. Figure C-1 below shows this spreadsheet program.

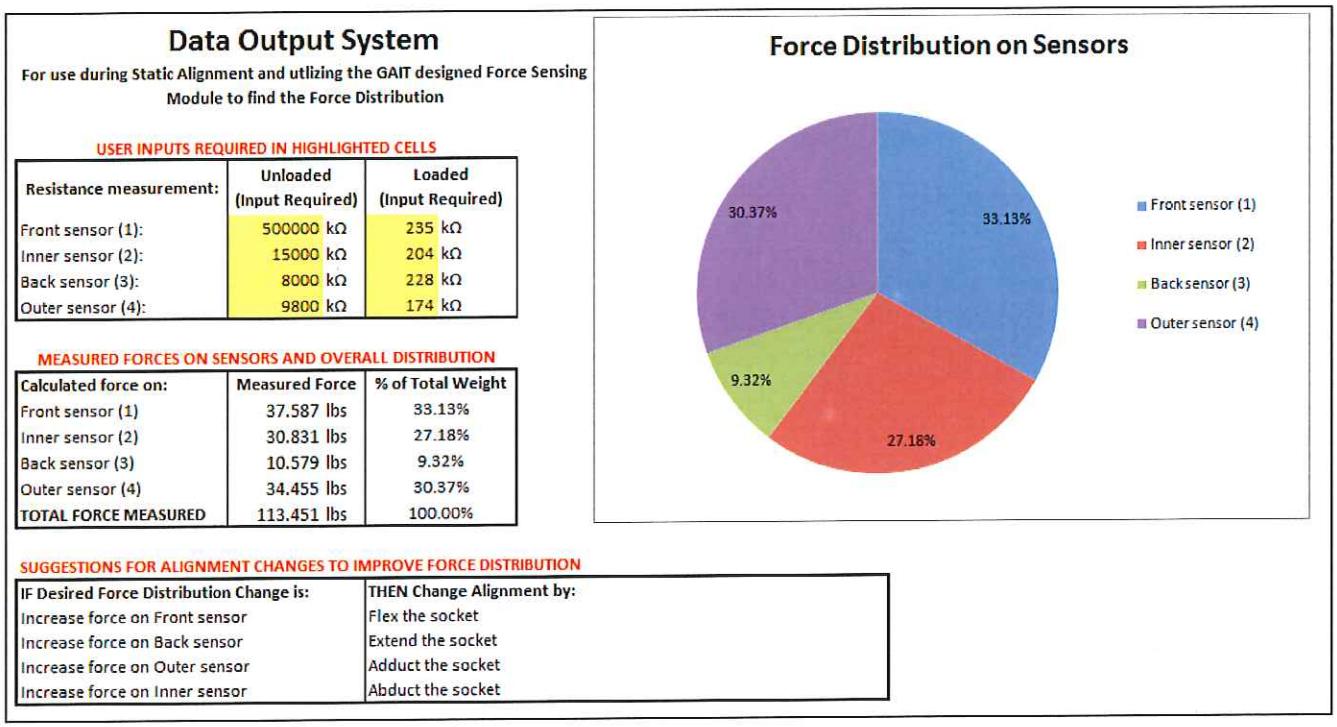

Data Output System

For use during Static Alignment and utlizing the GAIT designed Force Sensing Module to find the Force Distribution

USER INPUTS REQUIRED IN HIGHLIGHTED CELLS

Resistance measurement:	Unloaded (Input Required)	Loaded (Input Required)
Front sensor (1):	500000 kΩ	235 kΩ
Inner sensor (2):	15000 kΩ	204 kΩ
Back sensor (3):	8000 kΩ	228 kΩ
Outer sensor (4):	9800 kΩ	174 kΩ

MEASURED FORCES ON SENSORS AND OVERALL DISTRIBUTION

Calculated force on:	Measured Force	% of Total Weight
Front sensor (1)	37.587 lbs	33.13%
Inner sensor (2)	30.831 lbs	27.18%
Back sensor (3)	10.579 lbs	9.32%
Outer sensor (4)	34.455 lbs	30.37%
TOTAL FORCE MEASURED	113.451 lbs	100.00%

SUGGESTIONS FOR ALIGNMENT CHANGES TO IMPROVE FORCE DISTRIBUTION

IF Desired Force Distribution Change is:	THEN Change Alignment by:
Increase force on Front sensor	Flex the socket
Increase force on Back sensor	Extend the socket
Increase force on Outer sensor	Adduct the socket
Increase force on Inner sensor	Abduct the socket

Figure E-1. Spreadsheet program for data output.

F Factorial Design of Experiments

Objective:

1) To identify the effect of changing one of the five variables on the forces experienced by the force measuring system.
2) Use the matrix to test both the computer model and the actual prototype output.

Dependent (Response) Variable: Force measured in the force measuring device prototype.

Independent Variables:

Factor 1: Weight of patient

Levels:	50 lbs	75 lbs	125lbs

Factor 2: Socket angle in the sagittal plane (front to back)

Levels:	extend 3°	bench	flex 3°

Factor3: Socket angle in the coronal plane (side to side)

Levels:	adduct 3°	bench	abduct 3°

For a function of five variables, each with a high and a low value, there are 3^3 possible combinations to be tested in experiments. The following test matrix describes the 27 possible combinations of these parameters. The tests will be completed both for a change made at the foot pyramid and a change made at the socket pyramid. The matrix will be tested for two complete cycles: one for the computer simulation and one for testing on the actual prototype.

Table F-1. Factorial design of experiments test matrix.

		Sagittal Plane (front to back)	Coronal Plane (side to side)
Test Number	Patient Weight (Load in lb)	Socket alignment	Socket alignment
1	50	extend (one turn)	adduct (one turn)
2	50	extend (one turn)	bench
3	50	extend (one turn)	abduct (one turn)
4	50	bench	adduct (one turn)
5	50	bench	bench
6	50	bench	abduct (one turn)
7	50	flex (one turn)	adduct (one turn)
8	50	flex (one turn)	bench
9	50	flex (one turn)	abduct (one turn)
10	75	extend (one turn)	adduct (one turn)
11	75	extend (one turn)	bench
12	75	extend (one turn)	abduct (one turn)
13	75	bench	adduct (one turn)
14	75	bench	bench
15	75	bench	abduct (one turn)
16	75	flex (one turn)	adduct (one turn)
17	75	flex (one turn)	bench
18	75	flex (one turn)	abduct (one turn)
19	125	extend (one turn)	adduct (one turn)
20	125	extend (one turn)	bench
21	125	extend (one turn)	abduct (one turn)
22	125	bench	adduct (one turn)
23	125	bench	bench
24	125	bench	abduct (one turn)
25	125	flex (one turn)	adduct (one turn)
26	125	flex (one turn)	bench
27	125	flex (one turn)	abduct (one turn)

G Effects Plots for Physical and Computer Simulation Data

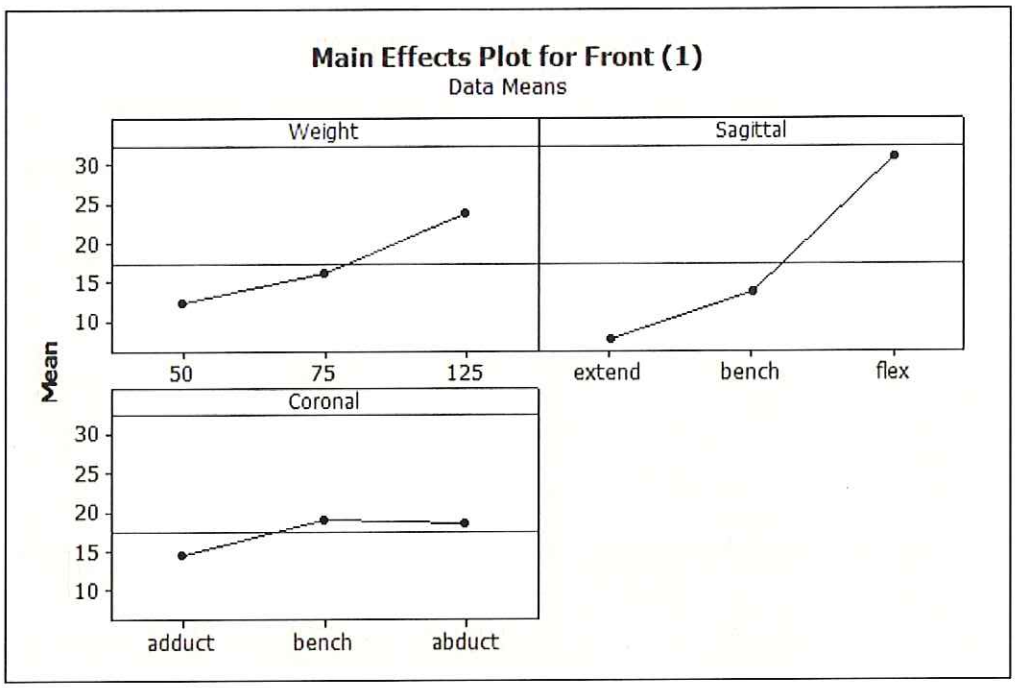

Figure G-1. Main Effects plot for front sensor for physical test data with bench values.

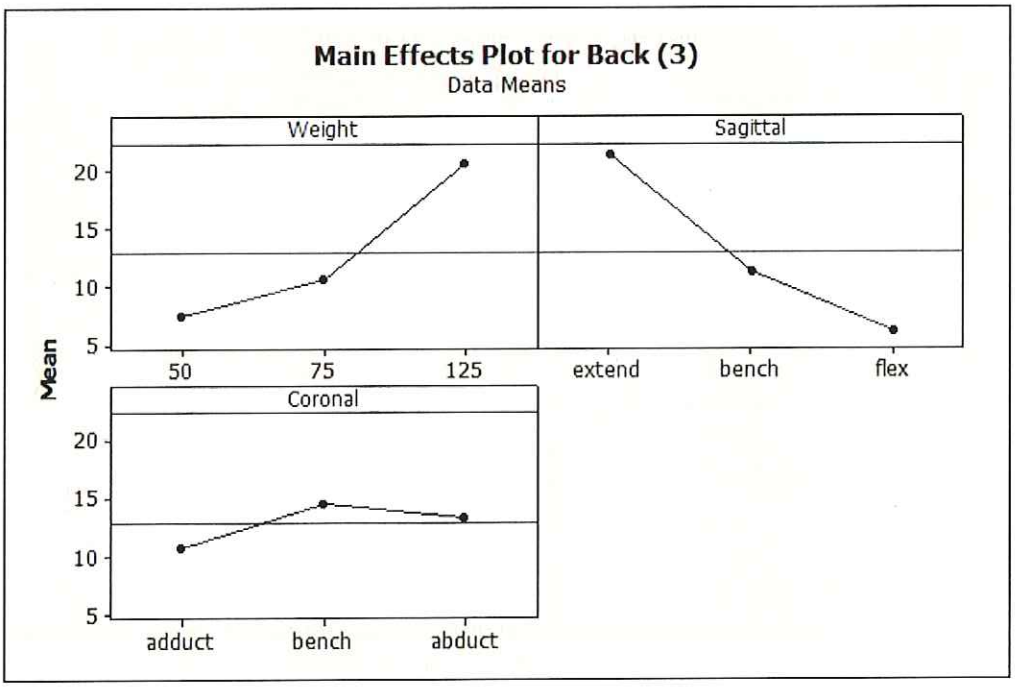

Figure G-2. Main Effects plot for back sensor for physical test data with bench values.

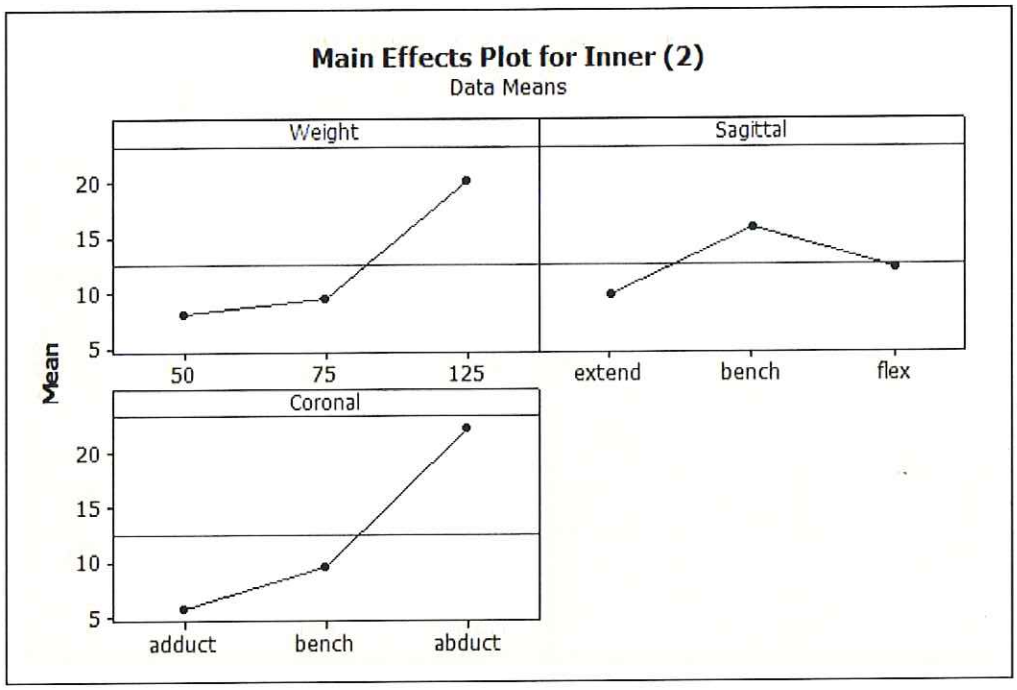

Figure G-3. Main Effects plot for inner sensor for physical test data with bench values.

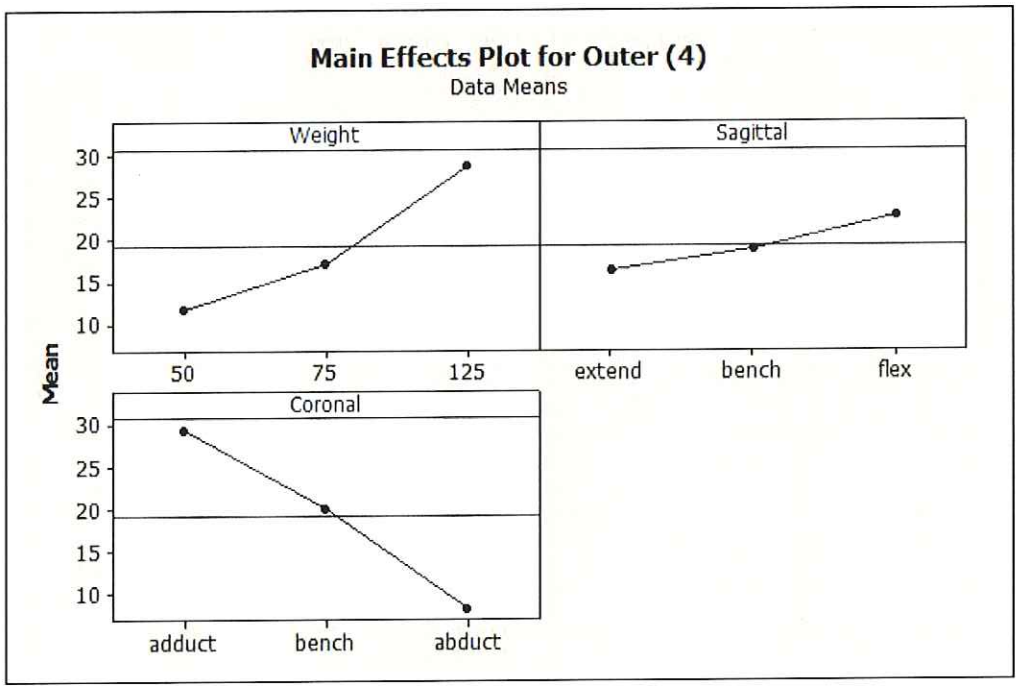

Figure G-4. Main Effects plot for outer sensor for physical test data with bench values.

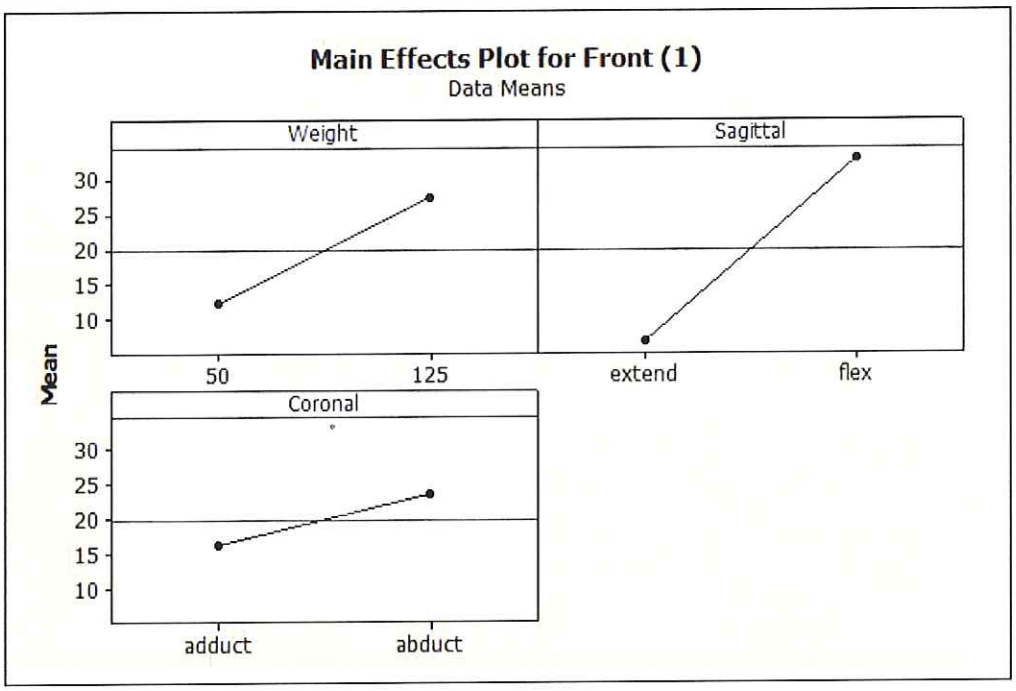

Figure G-5. Main Effects plot for front sensor for physical test data without bench.

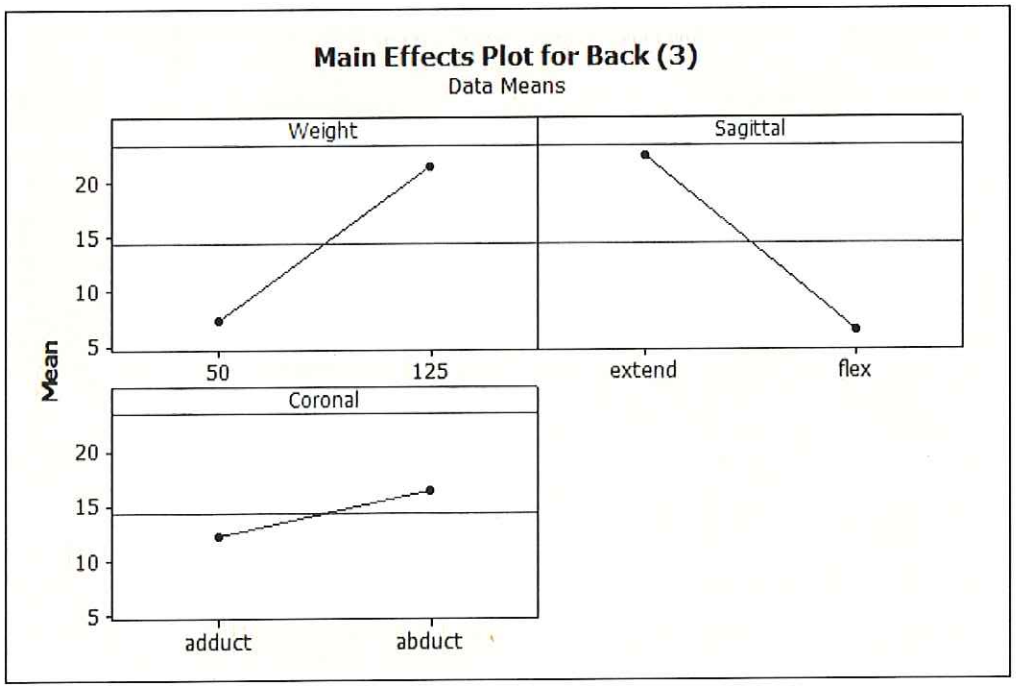

Figure G-6. Main Effects plot for back sensor for physical test data without bench.

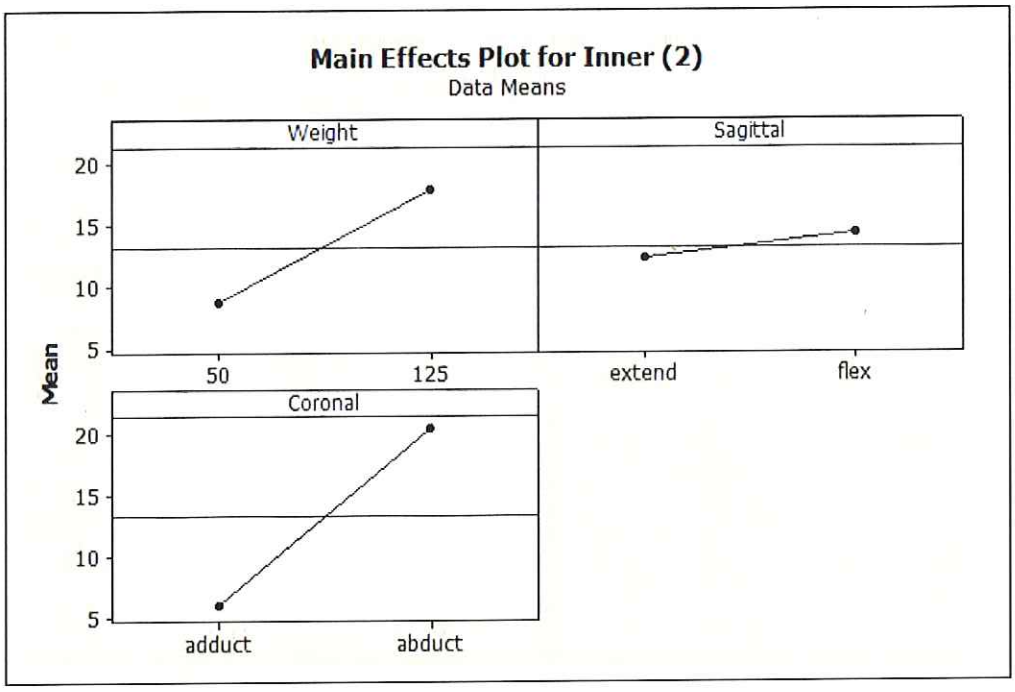

Figure G-7. Main Effects plot for inner sensor for physical test data without bench.

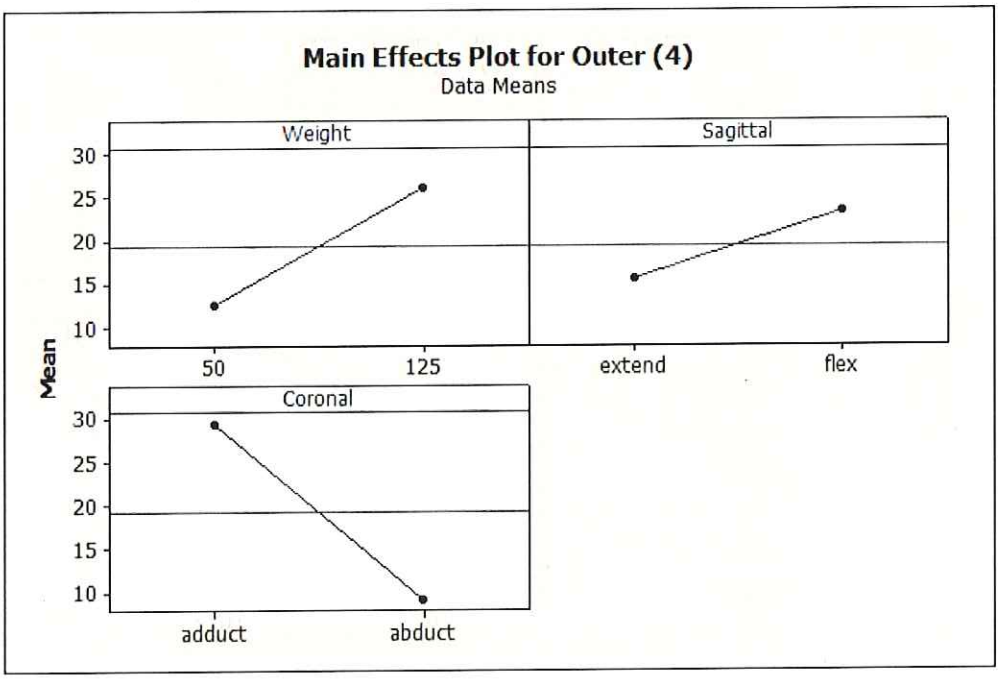

Figure G-8. Main Effects plot for outer sensor for physical test data without bench.

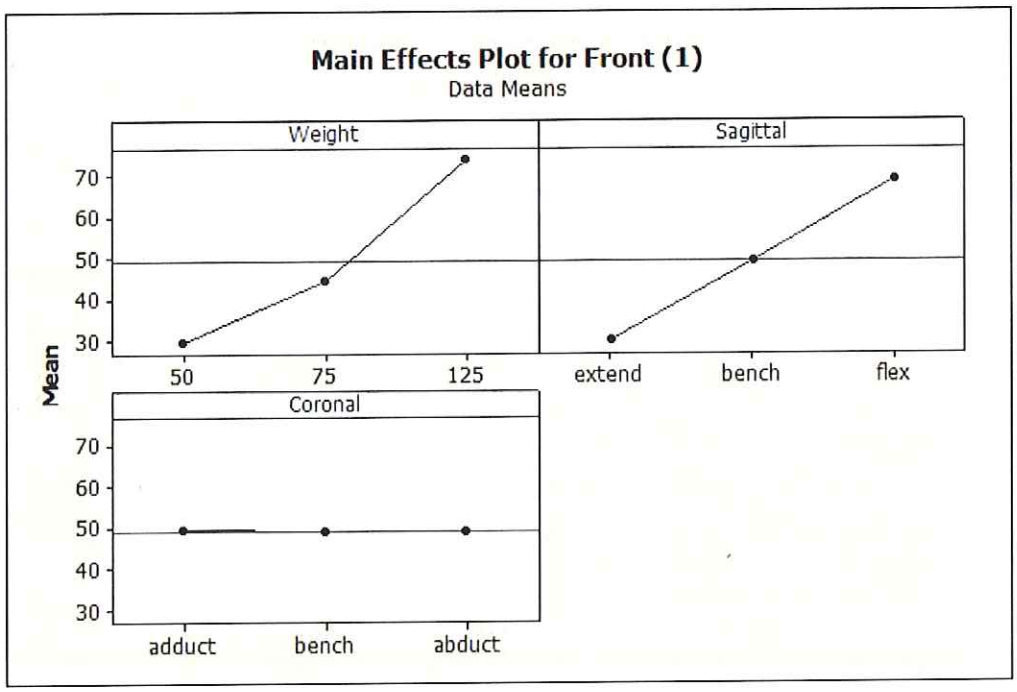

Figure G-9. Main Effects plot for front sensor for ProMechanica test data with bench.

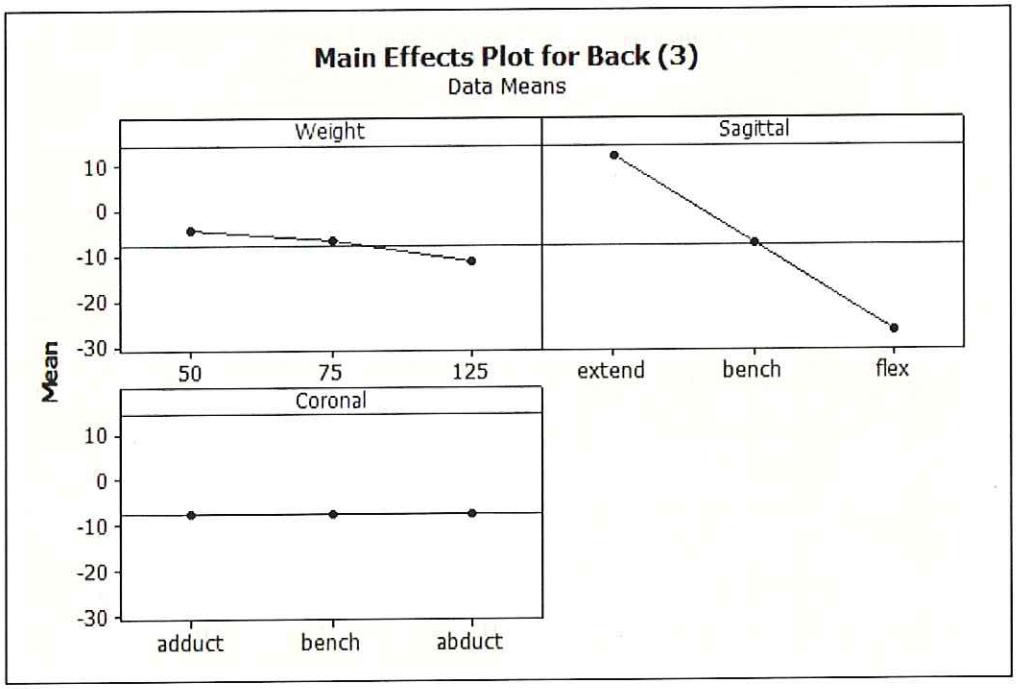

Figure G-10. Main Effects plot for back sensor for ProMechanica test data with bench.

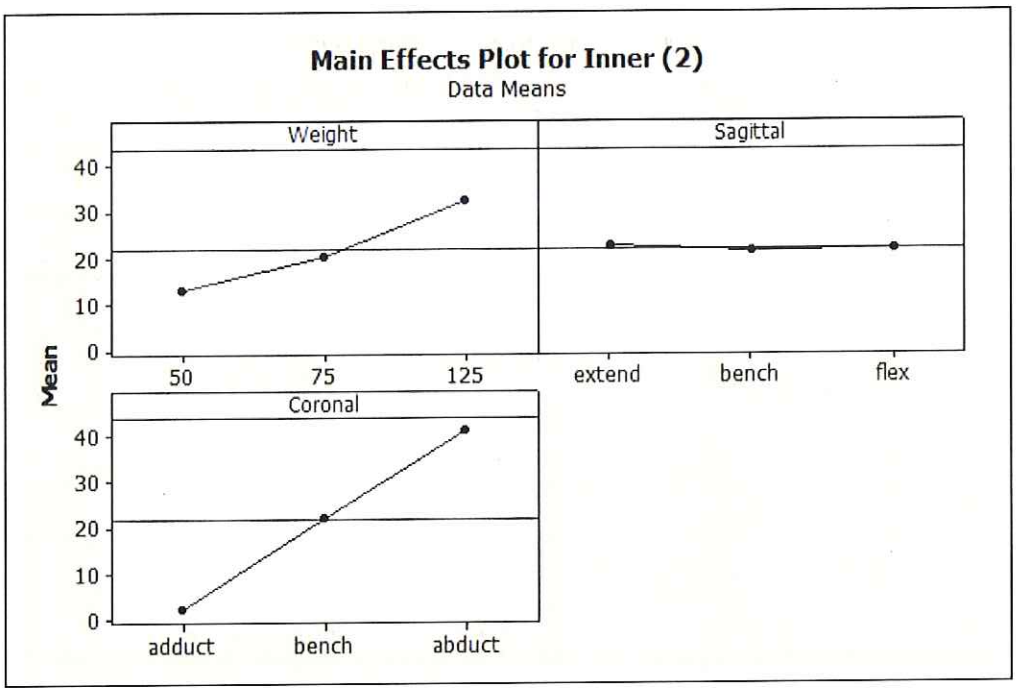

Figure G-11. Main Effects plot for inner sensor for ProMechanica test data with bench.

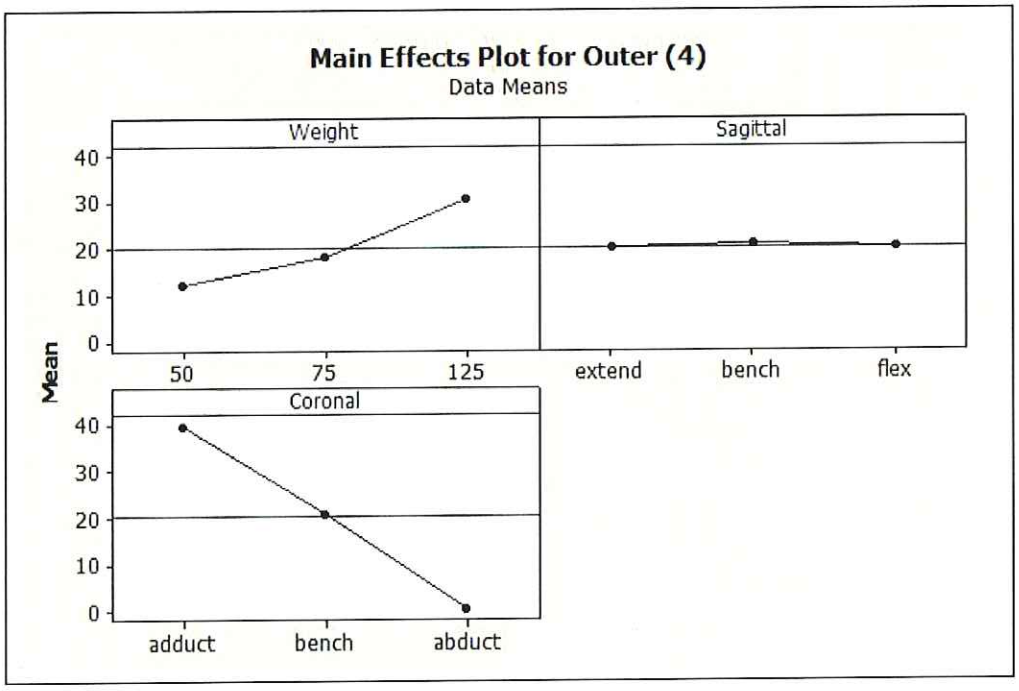

Figure G-12. Main Effects plot for outer sensor for ProMechanica test data with bench.

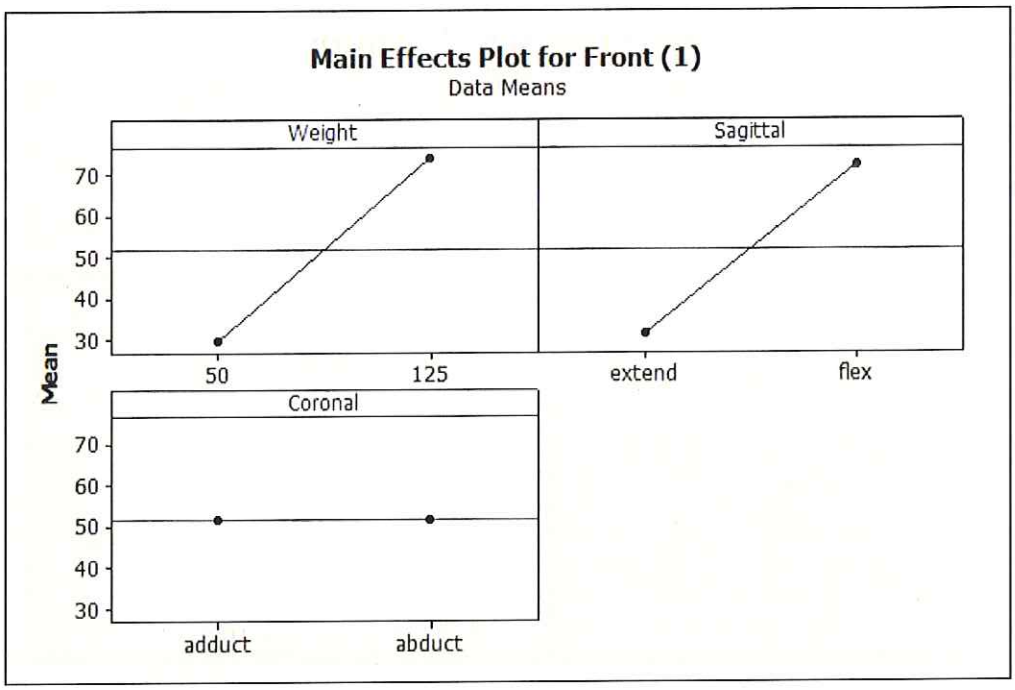

Figure G-13. Main Effects plot for front sensor for ProMechanica test data without bench.

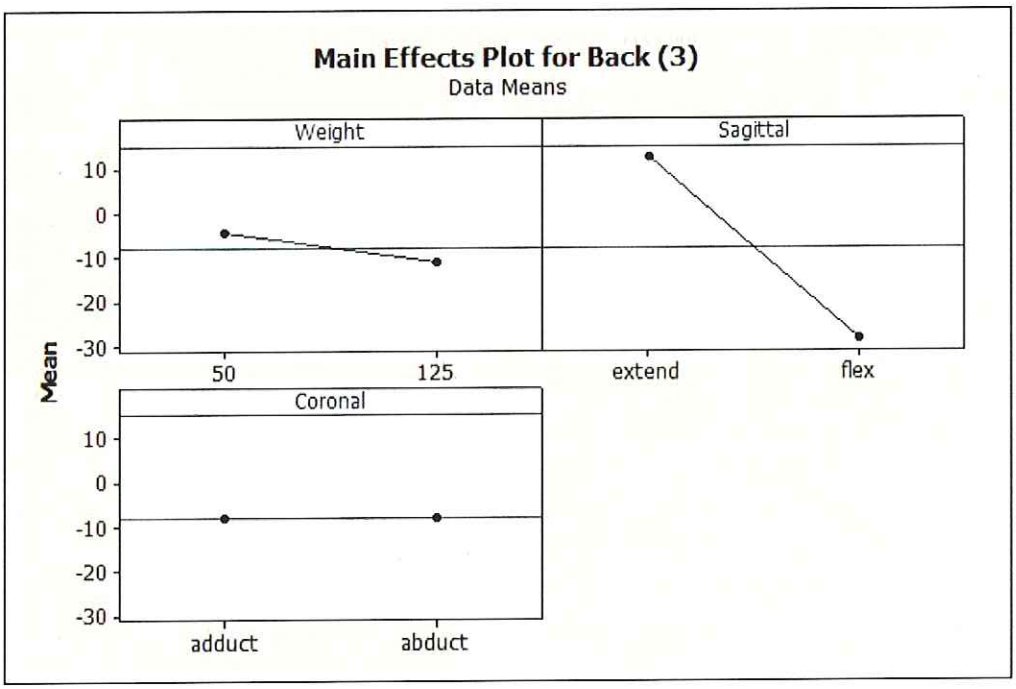

Figure G-14. Main Effects plot for back sensor for ProMechanica test data without bench.

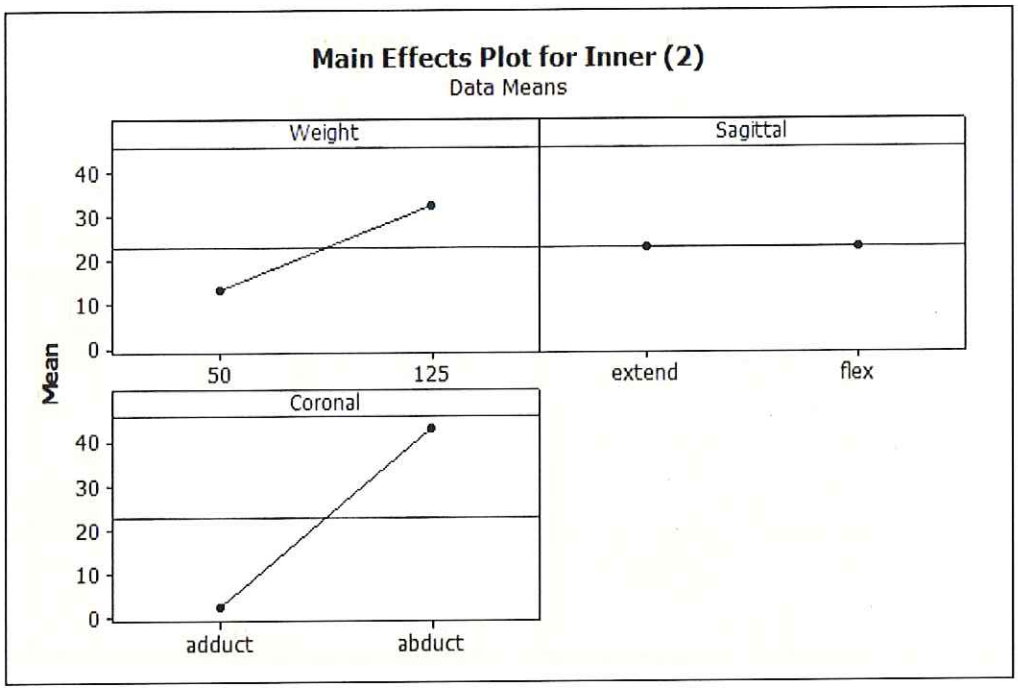

Figure G-15. Main Effects plot for inner sensor for ProMechanica test data without bench.

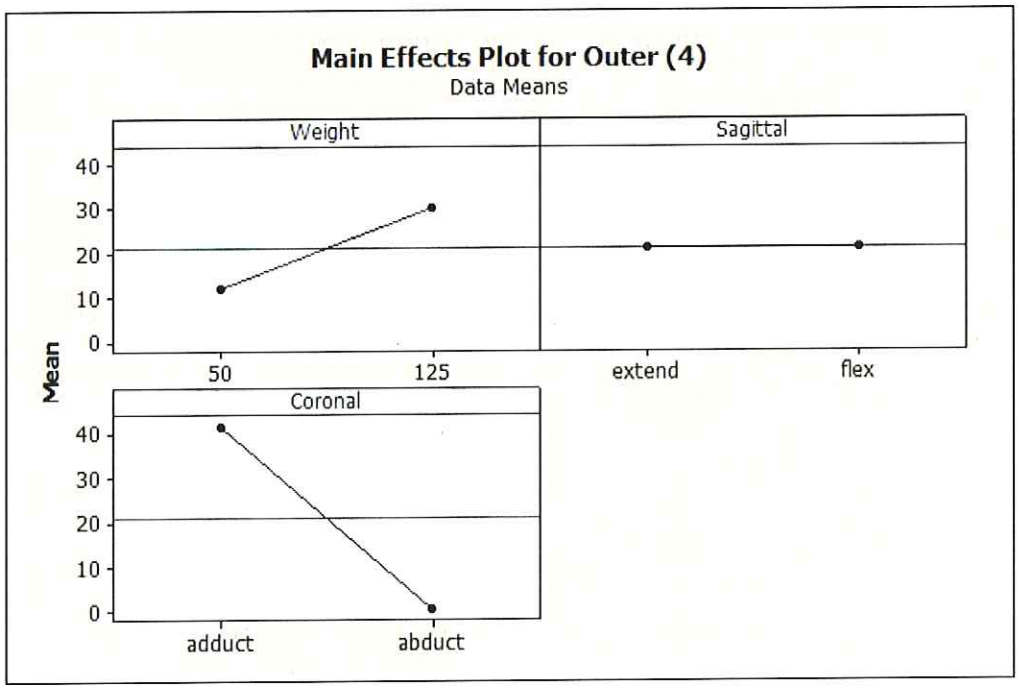

Figure G-16. Main Effects plot for outer sensor for ProMechanica test data without bench.

H Minitab Analysis Results (ANOVA and Prediction Equations)

Minitab Analysis for Physical Test Data Including Center Points (3-level)

General Linear Model: Front (1), Inner (2), ... versus Weight, Sagittal, ...

```
Factor    Type   Levels  Values
Weight    fixed       3  50, 75, 125
Sagittal  fixed       3  extend, bench, flex
Coronal   fixed       3  adduct, bench, abduct


Analysis of Variance for Front (1), using Adjusted SS for Tests

Source                   DF    Seq SS   Adj SS   Adj MS       F      P
Weight                    2   1221.61  1221.61   610.81   28.52  0.000
Sagittal                  2   5290.68  5290.68  2645.34  123.54  0.000
Coronal                   2    219.33   219.33   109.67    5.12  0.013
Weight*Sagittal           4   2788.09  2788.09   697.02   32.55  0.000
Weight*Coronal            4    202.48   202.48    50.62    2.36  0.078
Sagittal*Coronal          4    496.67   496.67   124.17    5.80  0.002
Weight*Sagittal*Coronal   8    404.56   404.56    50.57    2.36  0.045
Error                    27    578.15   578.15    21.41
Total                    53  11201.57


S = 4.62742   R-Sq = 94.84%   R-Sq(adj) = 89.87%


Unusual Observations for Front (1)

Obs  Front (1)      Fit  SE Fit  Residual  St Resid
 23    11.2880  17.9880  3.2721   -6.7000     -2.05 R
 25    22.3750  33.9435  3.2721  -11.5685     -3.54 R
 50    24.6880  17.9880  3.2721    6.7000      2.05 R
 52    45.5120  33.9435  3.2721   11.5685      3.54 R

R denotes an observation with a large standardized residual.


Analysis of Variance for Inner (2), using Adjusted SS for Tests

Source                   DF   Seq SS   Adj SS   Adj MS      F      P
Weight                    2  1558.44  1558.44   779.22  38.49  0.000
Sagittal                  2   331.78   331.78   165.89   8.19  0.002
Coronal                   2  2678.90  2678.90  1339.45  66.16  0.000
Weight*Sagittal           4   403.38   403.38   100.84   4.98  0.004
Weight*Coronal            4  1952.45  1952.45   488.11  24.11  0.000
Sagittal*Coronal          4   449.24   449.24   112.31   5.55  0.002
Weight*Sagittal*Coronal   8   489.44   489.44    61.18   3.02  0.015
Error                    27   546.64   546.64    20.25
Total                    53  8410.27


S = 4.49956   R-Sq = 93.50%   R-Sq(adj) = 87.24%


Unusual Observations for Inner (2)
```

Obs	Inner (2)	Fit	SE Fit	Residual	St Resid
23	5.9510	17.0125	3.1817	-11.0615	-3.48 R
26	24.5870	16.2720	3.1817	8.3150	2.61 R
50	28.0740	17.0125	3.1817	11.0615	3.48 R
53	7.9570	16.2720	3.1817	-8.3150	-2.61 R

R denotes an observation with a large standardized residual.

Analysis of Variance for Back (3), using Adjusted SS for Tests

Source	DF	Seq SS	Adj SS	Adj MS	F	P
Weight	2	1662.17	1662.17	831.08	63.53	0.000
Sagittal	2	2192.87	2192.87	1096.44	83.82	0.000
Coronal	2	133.37	133.37	66.69	5.10	0.013
Weight*Sagittal	4	830.97	830.97	207.74	15.88	0.000
Weight*Coronal	4	227.43	227.43	56.86	4.35	0.008
Sagittal*Coronal	4	67.83	67.83	16.96	1.30	0.296
Weight*Sagittal*Coronal	8	107.01	107.01	13.38	1.02	0.443
Error	27	353.19	353.19	13.08		
Total	53	5574.84				

S = 3.61676 R-Sq = 93.66% R-Sq(adj) = 87.56%

Unusual Observations for Back (3)

Obs	Back (3)	Fit	SE Fit	Residual	St Resid
20	48.2230	40.2845	2.5574	7.9385	3.10 R
47	32.3460	40.2845	2.5574	-7.9385	-3.10 R

R denotes an observation with a large standardized residual.

Analysis of Variance for Outer (4), using Adjusted SS for Tests

Source	DF	Seq SS	Adj SS	Adj MS	F	P
Weight	2	2745.16	2745.16	1372.58	30.36	0.000
Sagittal	2	391.74	391.74	195.87	4.33	0.023
Coronal	2	4085.87	4085.87	2042.94	45.19	0.000
Weight*Sagittal	4	266.75	266.75	66.69	1.48	0.237
Weight*Coronal	4	1481.29	1481.29	370.32	8.19	0.000
Sagittal*Coronal	4	136.84	136.84	34.21	0.76	0.562
Weight*Sagittal*Coronal	8	356.00	356.00	44.50	0.98	0.469
Error	27	1220.69	1220.69	45.21		
Total	53	10684.34				

S = 6.72390 R-Sq = 88.57% R-Sq(adj) = 77.57%

Unusual Observations for Outer (4)

Obs	Outer (4)	Fit	SE Fit	Residual	St Resid
23	42.0290	29.1135	4.7545	12.9155	2.72 R
26	56.2850	42.2095	4.7545	14.0755	2.96 R
50	16.1980	29.1135	4.7545	-12.9155	-2.72 R
53	28.1340	42.2095	4.7545	-14.0755	-2.96 R

R denotes an observation with a large standardized residual.

Minitab Analysis for Physical Test Data Excluding Center Points (2-level)

Results for: physical data without bench.MTW

Factorial Fit: Front (1), Inner (2), Back (3), Outer (4)

Factorial Fit: Front (1) versus Weight, Sagittal, Coronal

Estimated Effects and Coefficients for Front (1) (coded units)

Term	Effect	Coef	SE Coef	T	P
Constant		19.835	1.536	12.92	0.000
Weight	15.028	7.514	1.536	4.89	0.001
Sagittal	26.257	13.129	1.536	8.55	0.000
Coronal	7.312	3.656	1.536	2.38	0.044
Weight*Sagittal	17.707	8.854	1.536	5.76	0.000
Weight*Coronal	8.236	4.118	1.536	2.68	0.028
Sagittal*Coronal	7.827	3.913	1.536	2.55	0.034
Weight*Sagittal*Coronal	7.401	3.700	1.536	2.41	0.043

S = 6.14310 PRESS = 1207.61
R-Sq = 95.10% R-Sq(pred) = 80.42% R-Sq(adj) = 90.82%

Analysis of Variance for Front (1) (coded units)

Source	DF	Seq SS	Adj SS	Adj MS	F	P
Main Effects	3	3875.0	3875.0	1291.67	34.23	0.000
2-Way Interactions	3	1770.6	1770.6	590.19	15.64	0.001
3-Way Interactions	1	219.1	219.1	219.09	5.81	0.043
Residual Error	8	301.9	301.9	37.74		
Pure Error	8	301.9	301.9	37.74		
Total	15	6166.6				

Unusual Observations for Front (1)

Obs	StdOrder	Front (1)	Fit	SE Fit	Residual	St Resid
4	4	22.3750	33.9435	4.3438	-11.5685	-2.66R
12	12	45.5120	33.9435	4.3438	11.5685	2.66R

R denotes an observation with a large standardized residual.

Estimated Coefficients for Front (1) using data in uncoded units

Term	Coef
Constant	2.30237
Weight	0.200375
Sagittal	-7.53004
Coronal	-5.95263
Weight*Sagittal	0.236098
Weight*Coronal	0.109815
Sagittal*Coronal	-4.72104
Weight*Sagittal*Coronal	0.0986783

Factorial Fit: Inner (2) versus Weight, Sagittal, Coronal

Estimated Effects and Coefficients for Inner (2) (coded units)

Term	Effect	Coef	SE Coef	T	P
Constant		13.2407	0.5181	25.56	0.000
Weight	9.0744	4.5372	0.5181	8.76	0.000
Sagittal	2.0659	1.0329	0.5181	1.99	0.081
Coronal	14.4654	7.2327	0.5181	13.96	0.000
Weight*Sagittal	0.6409	0.3204	0.5181	0.62	0.553
Weight*Coronal	10.6734	5.3367	0.5181	10.30	0.000
Sagittal*Coronal	1.7174	0.8587	0.5181	1.66	0.136
Weight*Sagittal*Coronal	1.0804	0.5402	0.5181	1.04	0.328

S = 2.07244 PRESS = 137.441
R-Sq = 97.97% R-Sq(pred) = 91.88% R-Sq(adj) = 96.19%

Analysis of Variance for Inner (2) (coded units)

Source	DF	Seq SS	Adj SS	Adj MS	F	P
Main Effects	3	1183.44	1183.44	394.479	91.85	0.000
2-Way Interactions	3	469.12	469.12	156.375	36.41	0.000
3-Way Interactions	1	4.67	4.67	4.669	1.09	0.328
Residual Error	8	34.36	34.36	4.295		
Pure Error	8	34.36	34.36	4.295		
Total	15	1691.59				

Estimated Coefficients for Inner (2) using data in uncoded units

Term	Coef
Constant	2.65392
Weight	0.120992
Sagittal	0.28525
Coronal	-5.21958
Weight*Sagittal	0.0085450
Weight*Coronal	0.142312
Sagittal*Coronal	-0.40175
Weight*Sagittal*Coronal	0.0144050

Factorial Fit: Back (3) versus Weight, Sagittal, Coronal

Estimated Effects and Coefficients for Back (3) (coded units)

Term	Effect	Coef	SE Coef	T	P
Constant		14.328	0.9541	15.02	0.000
Weight	14.237	7.118	0.9541	7.46	0.000
Sagittal	-16.166	-8.083	0.9541	-8.47	0.000
Coronal	4.149	2.075	0.9541	2.17	0.061
Weight*Sagittal	-10.569	-5.285	0.9541	-5.54	0.001
Weight*Coronal	3.562	1.781	0.9541	1.87	0.099
Sagittal*Coronal	-2.210	-1.105	0.9541	-1.16	0.280
Weight*Sagittal*Coronal	-1.734	-0.867	0.9541	-0.91	0.390

S = 3.81631 PRESS = 466.055
R-Sq = 95.47% R-Sq(pred) = 81.87% R-Sq(adj) = 91.50%

Analysis of Variance for Back (3) (coded units)

Source	DF	Seq SS	Adj SS	Adj MS	F	P
Main Effects	3	1924.95	1924.95	641.65	44.06	0.000
2-Way Interactions	3	517.10	517.10	172.37	11.83	0.003
3-Way Interactions	1	12.02	12.02	12.02	0.83	0.390
Residual Error	8	116.51	116.51	14.56		
Pure Error	8	116.51	116.51	14.56		
Total	15	2570.58				

Estimated Coefficients for Back (3) using data in uncoded units

Term	Coef
Constant	-2.28196
Weight	0.189827
Sagittal	4.24762
Coronal	-2.08088
Weight*Sagittal	-0.140920
Weight*Coronal	0.0474900
Sagittal*Coronal	0.91771
Weight*Sagittal*Coronal	-0.0231167

Factorial Fit: Outer (4) versus Weight, Sagittal, Coronal

Estimated Effects and Coefficients for Outer (4) (coded units)

Term	Effect	Coef	SE Coef	T	P
Constant		19.29	1.033	18.68	0.000
Weight	13.66	6.83	1.033	6.61	0.000
Sagittal	7.69	3.84	1.033	3.72	0.006
Coronal	-20.40	-10.20	1.033	-9.88	0.000
Weight*Sagittal	4.02	2.01	1.033	1.94	0.088
Weight*Coronal	-11.51	-5.76	1.033	-5.57	0.001
Sagittal*Coronal	-3.41	-1.70	1.033	-1.65	0.137
Weight*Sagittal*Coronal	1.40	0.70	1.033	0.68	0.517

S = 4.13075 PRESS = 546.020
R-Sq = 96.02% R-Sq(pred) = 84.09% R-Sq(adj) = 92.54%

Analysis of Variance for Outer (4) (coded units)

Source	DF	Seq SS	Adj SS	Adj MS	F	P
Main Effects	3	2647.17	2647.17	882.389	51.71	0.000
2-Way Interactions	3	641.01	641.01	213.671	12.52	0.002
3-Way Interactions	1	7.86	7.86	7.857	0.46	0.517
Residual Error	8	136.50	136.50	17.063		
Pure Error	8	136.50	136.50	17.063		
Total	15	3432.54				

Unusual Observations for Outer (4)

Obs	StdOrder	Outer (4)	Fit	SE Fit	Residual	St Resid
8	8	7.1310	15.0205	2.9209	-7.8895	-2.70R
16	16	22.9100	15.0205	2.9209	7.8895	2.70R

R denotes an observation with a large standardized residual.

Estimated Coefficients for Outer (4) using data in uncoded units

Term	Coef
Constant	3.35579
Weight	0.182157
Sagittal	-0.84112
Coronal	3.23113
Weight*Sagittal	0.0535500
Weight*Coronal	-0.153480
Sagittal*Coronal	-3.33946
Weight*Sagittal*Coronal	0.0186867

Minitab Analysis for Computer Simulation Data Including Center Points (3-level)

Results for: promechanica data worksheet.MTW

General Linear Model: Front (1), Inner (2), ... versus Weight, Sagittal, ...

```
Factor    Type   Levels  Values
Weight    fixed       3  50, 75, 125
Sagittal  fixed       3  extend, bench, flex
Coronal   fixed       3  adduct, bench, abduct


Analysis of Variance for Front (1), using Adjusted SS for Tests

Source                   DF   Seq SS   Adj SS  Adj MS    F  P
Weight                    2  18304.3  18304.3  9152.2  **
Sagittal                  2  13758.5  13758.5  6879.3  **
Coronal                   2      0.1      0.1     0.0  **
Weight*Sagittal           4   1926.2   1926.2   481.5  **
Weight*Coronal            4      0.0      0.0     0.0  **
Sagittal*Coronal          4      0.4      0.4     0.1  **
Weight*Sagittal*Coronal   8      0.1      0.1     0.0  **
Error                    27      0.0      0.0     0.0
Total                    53  33989.6

** Denominator of F-test is zero.


S = 5.951247E-15   R-Sq = 100.00%   R-Sq(adj) = 100.00%


Analysis of Variance for Inner (2), using Adjusted SS for Tests

Source                   DF    Seq SS    Adj SS   Adj MS    F  P
Weight                    2   3551.93   3551.93  1775.97  **
Sagittal                  2      0.37      0.37     0.19  **
Coronal                   2  13817.80  13817.80  6908.90  **
Weight*Sagittal           4      0.05      0.05     0.01  **
Weight*Coronal            4   1934.49   1934.49   483.62  **
Sagittal*Coronal          4      0.52      0.52     0.13  **
Weight*Sagittal*Coronal   8      0.07      0.07     0.01  **
Error                    27      0.00      0.00     0.00
Total                    53  19305.24

** Denominator of F-test is zero.


S = 4.793166E-15   R-Sq = 100.00%   R-Sq(adj) = 100.00%


Analysis of Variance for Back (3), using Adjusted SS for Tests

Source                   DF    Seq SS    Adj SS   Adj MS    F  P
Weight                    2    437.06    437.06   218.53  **
Sagittal                  2  13707.71  13707.71  6853.85  **
Coronal                   2      0.11      0.11     0.05  **
Weight*Sagittal           4   1919.08   1919.08   479.77  **
Weight*Coronal            4      0.02      0.02     0.00  **
Sagittal*Coronal          4      0.72      0.72     0.18  **
Weight*Sagittal*Coronal   8      0.10      0.10     0.01  **
Error                    27      0.00      0.00     0.00
```

Total 53 16064.79

** Denominator of F-test is zero.

S = 4.182656E-15 R-Sq = 100.00% R-Sq(adj) = 100.00%

Analysis of Variance for Outer (4), using Adjusted SS for Tests

Source	DF	Seq SS	Adj SS	Adj MS	F	P
Weight	2	3045.48	3045.48	1522.74	**	
Sagittal	2	0.15	0.15	0.07	**	
Coronal	2	13787.98	13787.98	6893.99	**	
Weight*Sagittal	4	0.02	0.02	0.01	**	
Weight*Coronal	4	1930.32	1930.32	482.58	**	
Sagittal*Coronal	4	0.78	0.78	0.20	**	
Weight*Sagittal*Coronal	8	0.11	0.11	0.01	**	
Error	27	0.00	0.00	0.00		
Total	53	18764.85				

** Denominator of F-test is zero.

S = 5.691185E-15 R-Sq = 100.00% R-Sq(adj) = 100.00%

Minitab Analysis for Computer Simulation Data Excluding Center Points (2-level)

Results for: PROMECHANICA DATA WITHOUT BENCH.MTW

Factorial Fit: Front (1), Inner (2), Back (3), Outer (4)

Factorial Fit: Front (1) versus Weight, Sagittal, Coronal

Estimated Effects and Coefficients for Front (1) (coded units)

Term	Effect	Coef	SE Coef	T	P
Constant		51.6804	0	*	*
Weight	44.2975	22.1487	0	*	*
Sagittal	40.9585	20.4793	0	*	*
Coronal	-0.0058	-0.0029	0	*	*
Weight*Sagittal	17.5536	8.7768	0	*	*
Weight*Coronal	-0.0025	-0.0012	0	*	*
Sagittal*Coronal	0.0320	0.0160	0	*	*
Weight*Sagittal*Coronal	0.0137	0.0069	0	*	*

S = 0 PRESS = 0
R-Sq = 100.00% R-Sq(pred) = 100.00% R-Sq(adj) = 100.00%

Analysis of Variance for Front (1) (coded units)

Source	DF	Seq SS	Adj SS	Adj MS	F	P
Main Effects	3	14559.5	14559.5	4853.16	*	*
2-Way Interactions	3	1232.5	1232.5	410.84	*	*
3-Way Interactions	1	0.0	0.0	0.00	*	*
Residual Error	8	0.0	0.0	0.00		
Pure Error	8	0.0	0.0	0.00		
Total	15	15792.0				

Estimated Coefficients for Front (1) using data in uncoded units

Term	Coef
Constant	8.33333E-06
Weight	0.590633
Sagittal	8.33333E-06
Coronal	1.52857E-15
Weight*Sagittal	0.234049
Weight*Coronal	-3.29000E-05
Sagittal*Coronal	1.94636E-15
Weight*Sagittal*Coronal	0.000182900

Factorial Fit: Inner (2) versus Weight, Sagittal, Coronal

Estimated Effects and Coefficients for Inner (2) (coded units)

Term	Effect	Coef	SE Coef	T	P
Constant		22.7413	0	*	*
Weight	19.4925	9.7462	0	*	*
Sagittal	0.1222	0.0611	0	*	*
Coronal	41.0552	20.5276	0	*	*

Weight*Sagittal	0.0523	0.0262	0	*	*
Weight*Coronal	17.5950	8.7975	0	*	*
Sagittal*Coronal	-0.0665	-0.0333	0	*	*
Weight*Sagittal*Coronal	-0.0285	-0.0143	0	*	*

S = 0 PRESS = 0
R-Sq = 100.00% R-Sq(pred) = 100.00% R-Sq(adj) = 100.00%

Analysis of Variance for Inner (2) (coded units)

Source	DF	Seq SS	Adj SS	Adj MS	F	P
Main Effects	3	8261.99	8261.99	2754.00	*	*
2-Way Interactions	3	1238.37	1238.37	412.79	*	*
3-Way Interactions	1	0.00	0.00	0.00	*	*
Residual Error	8	0.00	0.00	0.00		
Pure Error	8	0.00	0.00	0.00		
Total	15	9500.37				

Estimated Coefficients for Inner (2) using data in uncoded units

Term	Coef
Constant	2.66667E-05
Weight	0.259900
Sagittal	2.30000E-05
Coronal	2.66667E-05
Weight*Sagittal	0.000697940
Weight*Coronal	0.234601
Sagittal*Coronal	2.36667E-05
Weight*Sagittal*Coronal	-3.80473E-04

Factorial Fit: Back (3) versus Weight, Sagittal, Coronal

Estimated Effects and Coefficients for Back (3) (coded units)

Term	Effect	Coef	SE Coef	T	P
Constant		-7.96	0	*	*
Weight	-6.82	-3.41	0	*	*
Sagittal	-41.08	-20.54	0	*	*
Coronal	-0.01	-0.01	0	*	*
Weight*Sagittal	-17.61	-8.80	0	*	*
Weight*Coronal	-0.01	-0.00	0	*	*
Sagittal*Coronal	-0.07	-0.04	0	*	*
Weight*Sagittal*Coronal	-0.03	-0.02	0	*	*

S = 0 PRESS = 0
R-Sq = 100.00% R-Sq(pred) = 100.00% R-Sq(adj) = 100.00%

Analysis of Variance for Back (3) (coded units)

Source	DF	Seq SS	Adj SS	Adj MS	F	P
Main Effects	3	6936.73	6936.73	2312.24	*	*
2-Way Interactions	3	1239.90	1239.90	413.30	*	*
3-Way Interactions	1	0.00	0.00	0.00	*	*
Residual Error	8	0.00	0.00	0.00		
Pure Error	8	0.00	0.00	0.00		

```
Total                15  8176.64
```

Estimated Coefficients for Back (3) using data in uncoded units

```
Term                            Coef
Constant                1.77636E-15
Weight                    -0.0909828
Sagittal                -7.10543E-15
Coronal                 1.66667E-06
Weight*Sagittal           -0.234747
Weight*Coronal          -7.17533E-05
Sagittal*Coronal        1.66667E-06
Weight*Sagittal*Coronal -4.01913E-04
```

Factorial Fit: Outer (4) versus Weight, Sagittal, Coronal

Estimated Effects and Coefficients for Outer (4) (coded units)

```
                                    SE
Term                    Effect    Coef  Coef  T  P
Constant                         21.06     0  *  *
Weight                   18.05    9.03     0  *  *
Sagittal                  0.00    0.00     0  *  *
Coronal                 -41.02  -20.51     0  *  *
Weight*Sagittal           0.00    0.00     0  *  *
Weight*Coronal          -17.58   -8.79     0  *  *
Sagittal*Coronal          0.10    0.05     0  *  *
Weight*Sagittal*Coronal   0.04    0.02     0  *  *
```

```
S = 0            PRESS = 0
R-Sq = 100.00%   R-Sq(pred) = 100.00%   R-Sq(adj) = 100.00%
```

Analysis of Variance for Outer (4) (coded units)

```
Source              DF   Seq SS   Adj SS   Adj MS  F  P
Main Effects         3  8034.13  8034.13  2678.04  *  *
2-Way Interactions   3  1236.31  1236.31   412.10  *  *
3-Way Interactions   1     0.01     0.01     0.01  *  *
Residual Error       8     0.00     0.00     0.00
  Pure Error         8     0.00     0.00     0.00
Total               15  9270.45
```

Estimated Coefficients for Outer (4) using data in uncoded units

```
Term                            Coef
Constant                8.25000E-07
Weight                     0.240677
Sagittal                -2.45833E-06
Coronal                 -8.41667E-07
Weight*Sagittal         1.57587E-05
Weight*Coronal            -0.234404
Sagittal*Coronal        2.54167E-06
Weight*Sagittal*Coronal  0.000578759
```

I Raw Test Data and Predicted Values

Table I-1. Raw Test Data and Predicted Values for Physical Force Measurement System.

	Values Generated with Prediction Equations					Physical Test Results (Raw Data)				
	Sagittal Plane		Coronal Plane			Sagittal Plane		Coronal Plane		
Test #	Front	Back	Inside	Outside	Total	Front	Back	Inside	Outside	Total
1	8.04626	10.00777	6.8075	16.90651	41.76804	10.744	6.806	6.674	12.141	36.365
2	8.04626	10.00777	8.70352	12.46364	39.22119	9.09	11.72	6.327	13.408	40.545
3	8.04626	10.00777	10.59954	8.02077	36.67434	6.908	10.446	8.533	10.791	36.678
4	12.32112	7.20939	6.8075	16.90651	43.24452	11.224	5.637	5.297	15.971	38.129
5	12.32112	7.20939	8.70352	12.46364	40.69767	10.612	7.497	7.643	11.695	37.447
6	12.32112	7.20939	10.59954	8.02077	38.15082	9.797	7.389	9.353	4.695	31.234
7	16.59598	4.41101	6.8075	16.90651	44.721	13.284	4.153	5.267	21.685	44.389
8	16.59598	4.41101	8.70352	12.46364	42.17415	17.859	4.121	6.794	9.531	38.305
9	16.59598	4.41101	10.59954	8.02077	39.6273	16.648	3.696	12.454	7.243	40.041
10	7.153185	18.276445	6.2745	25.297435	57.001565	13.563	12.509	5.951	18.679	50.702
11	7.153185	18.276445	11.72832	17.017565	54.175515	6.176	16.478	7.222	15.58	45.456
12	7.153185	18.276445	17.18214	8.737695	51.349465	6.609	15.282	12.332	7.895	42.118
13	17.330495	11.955065	6.2745	25.297435	60.857495	14.133	9.93	5.372	22.373	51.808
14	17.330495	11.955065	11.72832	17.017565	58.031445	18.956	6.528	9.672	13.167	48.323
15	17.330495	11.955065	17.18214	8.737695	55.205395	13.073	12.923	12.525	10.563	49.084
16	27.507805	5.633685	6.2745	25.297435	64.713425	16.366	6.023	5.277	37.284	64.95
17	27.507805	5.633685	11.72832	17.017565	61.887375	33.509	4.704	12.927	10.212	61.352
18	27.507805	5.633685	17.18214	8.737695	59.061325	28.293	3.626	14.289	11.96	58.168
19	5.367035	34.813795	5.2085	42.079285	87.468615	5.193	24.214	5.246	35.906	70.559
20	5.367035	34.813795	17.77792	26.125415	84.084165	5.201	48.223	6.077	22.776	82.277
21	5.367035	34.813795	30.34734	10.171545	80.699715	5.68	39.069	25.217	5.126	75.092
22	27.349245	21.446415	5.2085	42.079285	96.083445	6.165	13.019	5.032	52.212	76.428
23	27.349245	21.446415	17.77792	26.125415	92.698995	11.288	26.756	5.951	42.029	86.024
24	27.349245	21.446415	30.34734	10.171545	89.314545	9.611	15.362	66.374	4.454	95.801
25	49.331455	8.079035	5.2085	42.079285	104.698275	22.375	7.773	4.783	48.712	83.643
26	49.331455	8.079035	17.77792	26.125415	101.313825	59.522	10.91	24.587	56.285	151.304
27	49.331455	8.079035	30.34734	10.171545	97.929375	64.855	14.732	30.687	7.131	117.405

	Values Generated with Prediction Equations					Physical Test Results (Raw Data)				
	Sagittal Plane		Coronal Plane			Sagittal Plane		Coronal Plane		
Test #	Front	Back	Inside	Outside	Total	Front	Back	Inside	Outside	Total
28	8.04626	10.00777	6.8075	16.90651	41.76804	6.698	12.146	6.153	13.189	38.186
29	8.04626	10.00777	8.70352	12.46364	39.22119	10.675	17.104	7.157	10.738	45.674
30	8.04626	10.00777	10.59954	8.02077	36.67434	7.835	10.633	10.604	6.388	35.46
31	12.32112	7.20939	6.8075	16.90651	43.24452	10.555	7.707	6.343	12.597	37.202
32	12.32112	7.20939	8.70352	12.46364	40.69767	11.384	6.211	6.916	14.196	38.707
33	12.32112	7.20939	10.59954	8.02077	38.15082	13.511	6.939	12.744	4.67	37.864
34	16.59598	4.41101	6.8075	16.90651	44.721	20.406	4.558	9.136	20.611	54.711
35	16.59598	4.41101	8.70352	12.46364	42.17415	17.292	2.618	7.424	13.94	41.274
36	16.59598	4.41101	10.59954	8.02077	39.6273	16.046	5.237	10.807	7.661	39.751
37	7.153185	18.276445	6.2745	25.297435	57.001565	11.024	17.906	5.524	29.359	63.813
38	7.153185	18.276445	11.72832	17.017565	54.175515	7.523	16.097	6.733	12.208	42.561
39	7.153185	18.276445	17.18214	8.737695	51.349465	6.176	17.414	11.44	12.579	47.609
40	17.330495	11.955065	6.2745	25.297435	60.857495	13.839	11.21	6.054	21.564	52.667
41	17.330495	11.955065	11.72832	17.017565	58.031445	13.944	12.338	6.304	22.457	55.043
42	17.330495	11.955065	17.18214	8.737695	55.205395	17.202	9.434	24.549	6.553	57.738
43	27.507805	5.633685	6.2745	25.297435	64.713425	15.834	7.371	5.377	25.088	53.67
44	27.507805	5.633685	11.72832	17.017565	61.887375	27.476	4.595	6.56	24.141	62.772
45	27.507805	5.633685	17.18214	8.737695	59.061325	25.468	5.895	12.469	8.019	51.851
46	5.367035	34.813795	5.2085	42.079285	87.468615	5.22	33.759	5.262	34.54	78.781
47	5.367035	34.813795	17.77792	26.125415	84.084165	7.033	32.346	9.62	25.016	74.015
48	5.367035	34.813795	30.34734	10.171545	80.699715	5.375	42.213	29.973	5.519	83.08
49	27.349245	21.446415	5.2085	42.079285	96.083445	19.082	3.998	5.322	59.278	87.68
50	27.349245	21.446415	17.77792	26.125415	92.698995	24.688	24.55	28.074	16.198	93.51
51	27.349245	21.446415	30.34734	10.171545	89.314545	13.984	13.48	60.872	3.561	91.897
52	49.331455	8.079035	5.2085	42.079285	104.698275	45.512	4.618	5.543	49.159	104.832
53	49.331455	8.079035	17.77792	26.125415	101.313825	51.121	8.517	7.957	28.134	95.729
54	49.331455	8.079035	30.34734	10.171545	97.929375	64.584	5.193	35.512	22.91	128.199

Table I-2. Raw Test Data and Predicted Values for ProMechanica Simulation.

	Values Generated with Prediction Equations					Simulation Test Results (Raw Data)				
	Sagittal Plane		Coronal Plane			Single-Pass Adaptive (ProMechanica)				
Test #	Front	Back	Inside	Outside	Total	Front	Back	Inside	Outside	Total
1	17.829	7.188	1.265	23.754	50.036	17.840	7.172	1.211	23.782	50.005
2	17.829	7.188	12.995	12.034	50.046	17.780	7.131	12.952	12.153	50.016
3	17.829	7.188	24.725	0.314	50.056	17.818	7.205	24.709	0.284	50.016
4	29.532	-4.549	1.265	23.754	50.002	29.595	-4.582	1.229	23.768	50.009
5	29.532	-4.549	12.995	12.034	50.011	29.402	-4.755	13.155	12.204	50.006
6	29.532	-4.549	24.725	0.314	50.021	29.459	-4.489	24.838	0.196	50.003
7	41.234	-16.286	1.265	23.754	49.967	41.227	-16.263	1.319	23.726	50.009
8	41.234	-16.286	12.995	12.034	49.977	41.348	-16.167	12.894	11.928	50.003
9	41.234	-16.286	24.725	0.314	49.986	41.242	-16.310	24.741	0.343	50.016
10	26.744	10.782	1.897	35.631	75.055	26.760	10.758	1.817	35.673	75.007
11	26.744	10.782	19.493	18.051	75.069	26.670	10.697	19.428	18.229	75.024
12	26.744	10.782	37.088	0.470	75.084	26.728	10.807	37.064	0.426	75.024
13	44.297	-6.824	1.897	35.631	75.002	44.393	-6.873	1.843	35.651	75.013
14	44.297	-6.824	19.493	18.051	75.017	44.104	-7.132	19.733	18.306	75.011
15	44.297	-6.824	37.088	0.470	75.032	44.188	-6.734	37.257	0.293	75.004
16	61.851	-24.430	1.897	35.631	74.950	61.840	-24.394	1.978	35.589	75.013
17	61.851	-24.430	19.493	18.051	74.965	62.022	-24.250	19.342	17.892	75.005
18	61.851	-24.430	37.088	0.470	74.980	61.862	-24.465	37.111	0.515	75.024
19	44.573	17.971	3.162	59.385	125.091	44.600	17.929	3.028	59.455	125.012
20	44.573	17.971	32.488	30.085	125.116	44.450	17.828	32.380	30.382	125.040
21	44.573	17.971	61.813	0.784	125.140	44.546	18.012	61.773	0.710	125.040
22	73.829	-11.373	3.162	59.385	125.004	73.988	-11.456	3.071	59.419	125.022
23	73.829	-11.373	32.488	30.085	125.028	73.506	-11.887	32.888	30.510	125.017
24	73.829	-11.373	61.813	0.784	125.053	73.647	-11.224	62.095	0.489	125.007
25	103.085	-40.716	3.162	59.385	124.917	103.067	-40.657	3.297	59.315	125.021
26	103.085	-40.716	32.488	30.085	124.941	103.370	-40.417	32.236	29.819	125.009
27	103.085	-40.716	61.813	0.784	124.966	103.104	-40.775	61.852	0.858	125.039